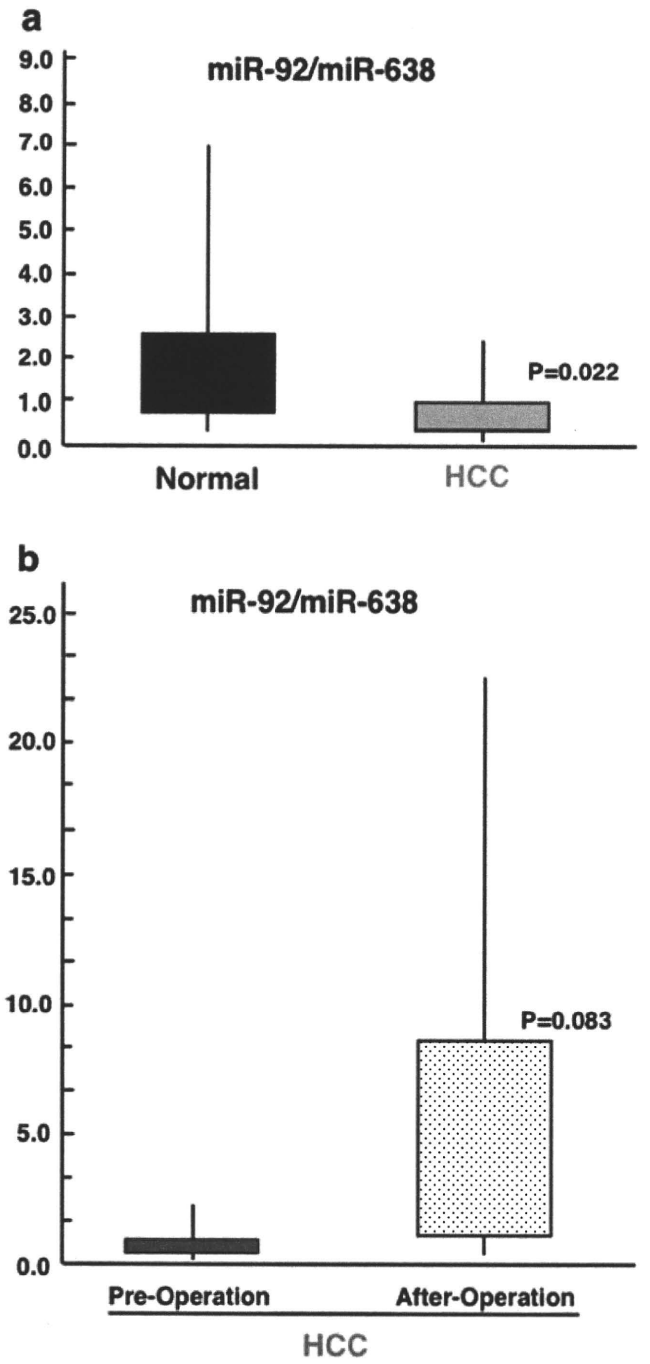


**Figure 4** Comparison of miR-92a levels in the plasmas from normal individuals and hepatocellular carcinoma (HCC) patients. (**a**) The ratios of miR-92a to miR-638 in the plasmas from normal donors and HCC patients were analyzed by *Taq*Man qRT-PCR. Student's *t*-test was used to determine statistical significance. (**b**) The ratios of miR-92a to miR-638 in the plasmas from HCC patients before and after tumor resection were analyzed by *Taq*Man qRT-PCR.

the expression of p63 in HCC by immunohistochemistry. However, we could not find the positive nuclear staining both in HCC and normal hepatocyte (data not shown). On the other hand, the miRanda software found 300 different genes that have putative miR-92a binding sites conserved among *Homo sapiens*, *Mus musculus*, and *Rattus norvegicus* at the 3′-UTR regions of their transcripts. Therefore, at least in HCC, there may be novel miR-92a targets that are involved in cancer cell proliferation.

In this report, we have revealed that the value of miR-92a/miR-638 in plasma has potential as a very sensitive marker for HCC. We found that the ratio of miR-92a to miR-638 in the plasma samples from the HCC patients were decreased compared with that from the normal donors (Fig. 4a). We did not find any differences in the values of the ratios between hepatitis B virus (HBV) infection and hepatitis C virus (HCV) infection (data not shown). On the other hand, we recently observed decrease of miR-92a in plasma samples of acute leukemia.[13] These results suggest that the decrease of the miR-92a/miR-638 level in human plasma may serve as a valuable diagnostic marker for not only acute leukemia but also solid tumors such as HCC. Moreover, we observed increase of miR-92a/miR-638 levels in the plasmas from the HCC patients after tumor resection (Fig. 4b). Thus, the miR-92a/miR-638 levels in human plasmas may also be a potential noninvasive follow up marker of HCC. To confirm this notion, a large number of plasma samples should be examined. Nevertheless, the levels of miR-92a/miR-638 promise to be an effective biomarker for malignant tumors. The physiological significance of the decrease of miR-92a in plasma is still unknown.

In summary, we have shown that miR-92a may be involved in HCC development. In addition, we have demonstrated that the ratio of miR-92a/miR-638 in blood is expected to be useful for diagnosis of HCC patients. This study may also provide useful information for further investigations of functional association between miRNAs and HCC.

## ACKNOWLEDGMENTS

This work was supported by Grants-in-Aids from the Ministry of Education, Culture, Sports, Science and Technology of Japan, the Ministry of Health, Labour and Welfare of Japan, Japan Health Sciences Foundation and a grant of Yamaguchi Endocrine Research Association and the grant of 'University-Industry Joint Research Project' for private universities as well as a matching fund subsidy from the MEXT (Ministry of Education, Culture, Sports, Science and Technology, 2007–2009). We thank Koji Fujita for his technical assistance and Satoko Aochi for her outstanding editorial assistance.

## REFERENCES

1 Mattick JS, Makunin IV. Non-coding RNA. *Hum Mol Genet* 2006; **15** (Spec No. 1): R17–29.

2 Esquela-Kerscher A, Slack FJ. Oncomirs—microRNAs with a role in cancer. *Nat Rev Cancer* 2006; **6**: 259–69.
3 Osada H, Takahashi T. MicroRNAs in biological processes and carcinogenesis. *Carcinogenesis* 2007; **28**: 2–12.
4 Hayashita Y, Osada H, Tatematsu Y *et al.* A polycistronic microRNA cluster, miR-17-92, is overexpressed in human lung cancers and enhances cell proliferation. *Cancer Res* 2005; **65**: 9628–32.
5 He L, Thomson JM, Hemann MT *et al.* A microRNA polycistron as a potential human oncogene. *Nature* 2005; **435**: 828–33.
6 Venturini L, Battmer K, Castoldi M *et al.* Expression of the miR-17-92 polycistron in chronic myeloid leukemia (CML) CD34+ cells. *Blood* 2007; **109**: 4399–405.
7 Uziel T, Karginov FV, Xie S *et al.* The miR-17-92 cluster collaborates with the Sonic Hedgehog pathway in medulloblastoma. *Proc Natl Acad Sci USA* 2009; **106**: 2812–17.
8 Diosdado B, van de Wiel MA, Terhaar Sive Droste JS *et al.* MiR-17-92 cluster is associated with 13q gain and c-myc expression during colorectal adenoma to adenocarcinoma progression. *Br J Cancer* 2009; **101**: 707–14.
9 Connolly E, Melegari M, Landgraf P *et al.* Elevated expression of the miR-17-92 polycistron and miR-21 in hepadnavirus-associated hepatocellular carcinoma contributes to the malignant phenotype. *Am J Pathol* 2008; **173**: 856–64.
10 Ventura A, Young AG, Winslow MM *et al.* Targeted deletion reveals essential and overlapping functions of the miR-17 through 92 family of miRNA clusters. *Cell* 2008; **132**: 875–86.
11 Manni I, Artuso S, Careccia S *et al.* The microRNA miR-92 increases proliferation of myeloid cells and by targeting p63 modulates the abundance of its isoforms. *FASEB J* 2009; **23**: 3957–66.
12 Bonauer A, Carmona G, Iwasaki M *et al.* MicroRNA-92a controls angiogenesis and functional recovery of ischemic tissues in mice. *Science* 2009; **324**: 1710–13.
13 Tanaka M, Oikawa K, Takanashi M *et al.* Down-regulation of miR-92 in human plasma is a novel marker for acute leukemia patients. *PLoS ONE* 2009; **4**: e5532.
14 Lohmann V, Korner F, Koch J, Herian U, Theilmann L, Bartenschlager R. Replication of subgenomic hepatitis C virus RNAs in a hepatoma cell line. *Science* 1999; **285**: 110–13.
15 Ikeda M, Abe K, Dansako H, Nakamura T, Naka K, Kato N. Efficient replication of a full-length hepatitis C virus genome, strain O, in cell culture, and development of a luciferase reporter system. *Biochem Biophys Res Commun* 2005; **329**: 1350–9.
16 Ikeda M, Abe K, Yamada M, Dansako H, Naka K, Kato N. Different anti-HCV profiles of statins and their potential for combination therapy with interferon. *Hepatology* 2006; **44**: 117–25.
17 Krutzfeldt J, Rajewsky N, Braich R *et al.* Silencing of microRNAs in vivo with 'antagomirs'. *Nature* 2005; **438**: 685–9.

*Journal of General Virology* (2010), **91**, 2080–2090 DOI 10.1099/vir.0.020552-0

# Hepatitis B virus polymerase inhibits RIG-I- and Toll-like receptor 3-mediated beta interferon induction in human hepatocytes through interference with interferon regulatory factor 3 activation and dampening of the interaction between TBK1/IKKε and DDX3

Shiyan Yu,[1,2]† Jieliang Chen,[1,2]† Min Wu,[2] Hui Chen,[1,2] Nobuyuki Kato[3] and Zhenghong Yuan[1,2,4]

**Correspondence**
Zhenghong Yuan
zhyuan@shaphc.org

[1]Key Laboratory of Medical Molecular Virology, Ministry of Education and Public Health, Shanghai Medical College, Fudan University, Shanghai 200032, PR China

[2]Shanghai Public Health Clinical Center affiliated to Fudan University, Shanghai 201508, PR China

[3]Department of Tumour Virology, Okayama University, Okayama 700-8558, Japan

[4]Institutes of Biomedical Sciences and Medical Microbiology, Fudan University, Shanghai 200032, PR China

Hepatitis B virus (HBV) infection remains one of the most serious health problems worldwide. Whilst studies have shown that HBV impairs interferon (IFN) production from dendritic cells in chronic hepatitis B patients, it remains unknown whether HBV inhibits IFN production in human hepatocytes. Using transient transfection assays in a primary human hepatocyte cell line (PH5CH8), this study demonstrated that HBV polymerase inhibits *IFN-β* promoter activity induced by Newcastle disease virus, Sendai virus or poly(I : C) in a dose-dependent manner, whilst ectopic expression of the HBV core and X proteins had no effect on *IFN-β* promoter activity. In addition, HBV polymerase blocked cellular IFN-β expression and consequent antiviral immunity revealed by an infection protection assay. Furthermore, overexpression of key molecules on the IFN-β induction axis, together with HBV polymerase, resulted in a block of *IFN-β* promoter activity triggered by RIG-I, IPS-1, TRIF, TBK1 and IKKε, but not by an IFN regulatory factor 3 dominant-positive mutant (IRF3-5D), suggesting that HBV polymerase prevents IFN-β expression at the TBK1/IKKε level. Further studies showed that HBV polymerase inhibited phosphorylation, dimerization and nuclear translocation of IRF3, in response to Sendai virus infection. Finally, it was shown that HBV polymerase-mediated dampening of the interaction between TBK1/IKKε and DDX3 may be involved in the inhibitory effect on IFN-β induction. Taken together, these findings reveal a novel role of HBV polymerase in HBV counteraction of IFN-β production in human hepatocytes.

Received 29 January 2010
Accepted 6 April 2010

## INTRODUCTION

Hepatitis B virus (HBV), one of many pathogens seriously jeopardizing global health, can establish persistent infection in the human liver and is closely associated with chronic hepatitis, cirrhosis and hepatocellular carcinoma (Ganem & Prince, 2004; Liaw & Chu, 2009). However, the underlying mechanism resulting in chronic hepatitis B infection has remained elusive. Human hepatocytes, the major target of HBV infection, are the only confirmed site of replication for the virus. It has been reported that hepatocytes have an innate immune response (Crispe, 2009; Lucifora *et al.*, 2010). Nevertheless, HBV has developed some sophisticated mechanisms to evade or subvert key aspects of the antiviral activity of liver cells (Foster *et al.*, 1991; Wu *et al.*, 2009).

The type I interferon (IFN) system, an indispensable part of the host innate immune response, exerts an immediate antiviral response through induction of numerous functional proteins against the virus life cycle and activates the adaptive immune response. Type I IFNs can be induced by a Toll-like receptor (TLR)- or RIG-I-like helicase (RLH)-

†These authors contributed equally to this work.

Data showing inhibition of IRF3 nuclear translocation and the involvement of DDX3 in inhibition of IFN-β induction by HBV polymerase are available with the online version of this paper.

mediated signalling pathway. The upstream pathways are distinct for these two different signals: TRIF is essential for a TLR3-induced IFN response, whilst IPS-1 is required for a RIG-I-induced IFN response. These two pathways converge at the level of TBK1/IKKε, which can phosphorylate IFN regulatory factor 3 (IRF3) and IRF7, two important transcriptional factors required for induction of type I IFNs (Takeuchi & Akira, 2009). In addition, it has been reported that the DEAD-box helicase DDX3 is also a crucial component in induction of type I IFNs that can contribute to activation of IRFs and ultimately the *IFN-β* promoter (Schröder *et al.*, 2008; Soulat *et al.*, 2008).

A growing body of evidence also suggests that HBV can eliminate type I IFNs. In chronic hepatitis B infection, there is a functional impairment of plasmacytoid dendritic cells, which are the predominant producers of IFN-α during virus infection (van der Molen *et al.*, 2004). In addition, it has been reported that hepatitis B virus surface antigen (HBsAg), hepatitis B virus e antigen (HBeAg) and HBV virions almost completely suppress TLR-mediated antiviral activity and cytokine induction in murine liver parenchymal cells, indicating that HBV can counteract the TLR-mediated innate immune response in the microenvironment surrounding the infection foci (Wu *et al.*, 2009). Although it is known that the RLH-mediated signalling pathway plays a critical role in the detection of invading pathogens and induction of IFN-β, little is known about whether and how HBV disturbs cytoplasmic RLH-mediated IFN-β induction in human hepatocytes.

In this paper, we identified HBV polymerase as a potent inhibitor of IFN-β induction in human hepatocytes. Expression of HBV polymerase led to inhibition of promoter activity and transcription of *IFN-β*, IFN-β expression and antiviral immunity in a primary hepatocytic cell line, PH5CH8. In addition, we demonstrated that HBV polymerase interfered with IFN-β induction at the TBK1/IKKε level. Furthermore, expression of HBV polymerase inhibited Sendai virus (SeV)-induced endogenous IRF3 phosphorylation, dimerization and nuclear translocation. Finally, our results showed that DDX3 may be involved in the inhibition of IFN-β induction by HBV polymerase.

## RESULTS

### Effects of HBV proteins on *IFN-β* promoter activity in human hepatocytes

In the HBV life cycle, three viral proteins (HBx, core and polymerase) can localize in the cellular cytoplasm (Seeger & Mason, 2000). To determine whether these viral proteins interfere with IFN-β induction, we performed a functional screen assay using an *IFN-β* promoter activity reporter system. Primary hepatocytic PH5CH8 cells capable of IFN-β induction in response to Newcastle disease virus (NDV), SeV or poly(I:C) were transfected with a construct for HBV polymerase, core or HBx. In parallel, hepatitis C virus (HCV) NS3/4A, a well-known inhibitor of IFN-β induction (Ferreon *et al.*, 2005; Li *et al.*, 2005c), was used as a positive control. Similar to HCV NS3/4A, HBV polymerase significantly repressed *IFN-β* promoter activity induced by infection of NDV, SeV and direct addition of poly(I:C) into the culture medium compared with empty vector control (Fig. 1a, left panel). In contrast, expression of the HBV core or HBx did not significantly reduce *IFN-β* promoter activity although their expression levels were slightly higher than HBV polymerase (Fig. 1a, right panel). These results indicated that HBV polymerase can be involved in manipulation of IFN-β induction by RIG-I or TLR3 in HBV infection.

To investigate further the effect of HBV polymerase on *IFN-β* promoter activity on a whole HBV genome scale, we compared the response of HepG2 cells harbouring wild-type HBV or polymerase-null HBV (HBV-ΔPol). Given that HepG2 cells are deficient in their response to extracellular poly(I:C) and have a diminished response to SeV infection (Li *et al.*, 2005a and our unpublished data), we co-transfected the cells with constructs expressing RIG-I, IPS-1 or TRIF, together with wild-type HBV or HBV-ΔPol. As expected, in the cells transfected with the wild-type HBV, *IFN-β* promoter activity stimulated by RIG-I, IPS-1 or TRIF was reduced when compared with that in cells lacking HBV polymerase expression (Fig. 1b–d).

To exclude the possibility of non-specific effects on *IFN-β* promoter activity, we examined whether HBV polymerase had an effect on the unrelated *p53* promoter activity. No inhibitory effect of HBV polymerase on the *p53* promoter was detected (Fig. 1e). Overall, these results strongly indicated that HBV polymerase interferes with IFN-β induction by both TLR3 and RIG-I signals.

### HBV polymerase inhibits promoter activity and expression of the *IFN-β* gene in human hepatocytes in a dose-dependent manner

To characterize further the inhibitory effect of HBV polymerase on IFN-β production in human hepatocytes, increasing amounts of HBV polymerase were transfected into PH5CH8 cells followed by NDV infection. *IFN-β* promoter activity induced by NDV was significantly decreased with increasing expression of HBV polymerase (Fig. 2a), indicating that HBV polymerase can inhibit *IFN-β* promoter activity in a dose-dependent manner. Similar results were also obtained with SeV infection and poly(I:C) treatment (data not shown).

In addition, we determined the effect of HBV polymerase on endogenous *IFN-β* transcription. Different amounts of HBV polymerase were transfected into PH5CH8 cells followed by NDV infection or direct addition of poly(I:C) into the culture medium, and the level of *IFN-β* mRNA was quantified using real-time PCR. As expected, the cells produced less *IFN-β* mRNA with increasing expression of HBV polymerase, indicating that HBV polymerase also

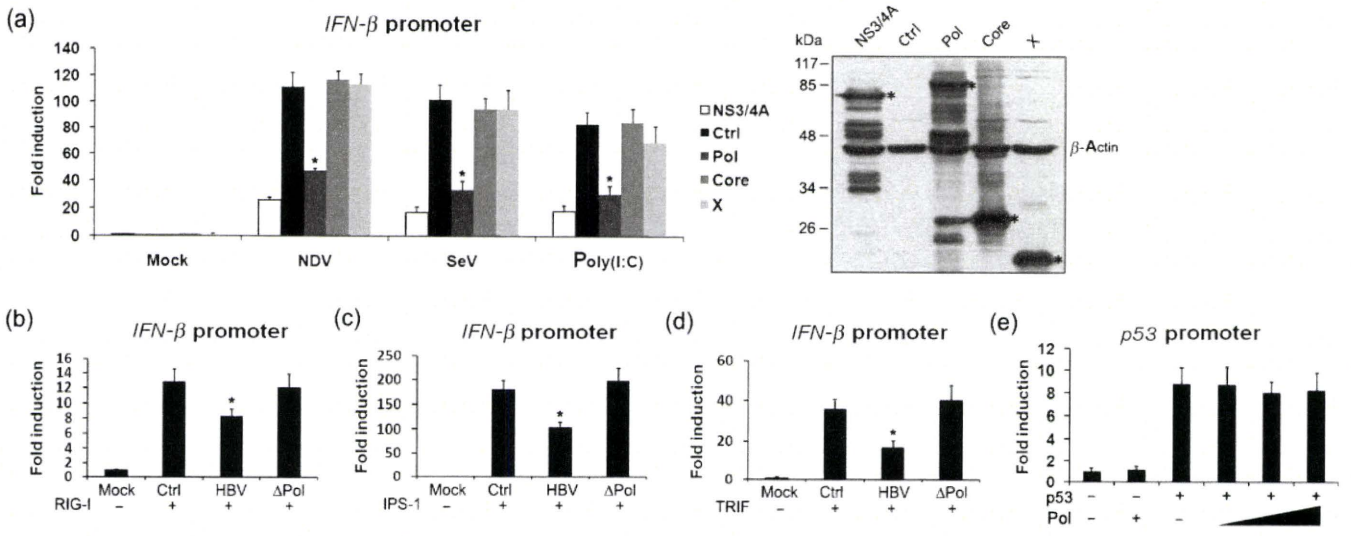


**Fig. 1.** HBV polymerase, but not core or HBx, inhibits RIG-I- and TLR3-induced *IFN-β* promoter activity. (a) PH5CH8 cells in a 48-well plate were co-transfected with pIFN-β-Luc, pRL-TK and 250 ng of plasmid encoding Flag-tagged HBV polymerase (Pol), HBV core, HBx (X) or HCV NS3/4A. After 36 h, the cells were infected with 100 haemagglutination units (HAU) NDV or SeV $ml^{-1}$, or stimulated with 50 μg poly(I : C) $ml^{-1}$, added directly to the culture medium for 12 h and then assayed for luciferase activity (left panel). Expression of the plasmids encoding the indicated proteins was detected by immunoblotting using anti-Flag antibody (right panel; asterisks indicate the relevant protein). (b–e) HepG2 cells in 24-well plates were co-transfected with pIFN-β-Luc, pRL-TK and either 500 ng wild-type HBV or HBV-ΔPol together with 50 ng RIG-I (b), IPS-1 (c) or TRIF (d). At 36 h post-transfection, cells were harvested for luciferase activity. *p53* promoter activity was detected in PH5CH8 cells co-transfected with 100 ng pp53–Luc and increasing amounts of HBV polymerase (e).

inhibits endogenous *IFN-β* gene transcription in a dose-dependent manner (Fig. 2b).

Furthermore, we examined the amount of IFN-β produced by PH5CH8 cells in the presence of HBV polymerase. PH5CH8 cells were transfected with the indicated amounts of HBV polymerase and then challenged by NDV infection. The results showed that IFN-β levels in the supernatant induced by NDV were inversely proportional to HBV polymerase expression levels (Fig. 2c), thus indicating that HBV polymerase inhibits IFN-β expression in PH5CH8 cells in a dose-dependent manner.

Taken together, these results indicated that HBV polymerase is a vital regulator that negatively modulates the production of IFN-β in human hepatocytes.

## HBV polymerase impairs IFN-β-mediated protective antiviral immunity

Blocking the spread of virus infection is one of the most important functions of IFN-β produced by infected cells. To address the effect of HBV polymerase on this function, we analysed the induced antiviral activity of PH5CH8 cells transfected with HBV polymerase through a virus infection protection assay (Fig. 3a). The antiviral activities of supernatants harvested from transfected PH5CH8 cells challenged with NDV were compared based on the extent of green fluorescent protein-tagged NDV (NDV–GFP) replication in Vero cells. Viral GFP expression was decreased in Vero cells pre-treated with the supernatant of NDV-treated PH5CH8 cells and IFN-α (Fig. 3b, lanes/panels 2 and 7), whereas GFP expression levels in Vero cells pre-treated with supernatant from the NS3/4A group was almost identical to the mock group (Fig. 3b, lanes/panels 1 and 6), suggesting that NS3/4A could abolish IFN-β expression in PH5CH8 cells challenged by NDV. In the HBV polymerase groups, the supernatants gradually lost the ability to block virus replication with increasing HBV polymerase expression (Fig. 3b, lanes/panels 3–5). These data indicated that the innate antiviral response in PH5CH8 cells was substantially decreased in the presence of HBV polymerase.

To test the possibility of other cytokines in the supernatant contributing to the antiviral effect, we further characterized the role of IFN-β in protective antiviral immunity in PH5CH8 cells using an IFN-β neutralizing antibody. When co-incubated with neutralizing antibody, the supernatant of PH5CH8 cells treated with NDV was deprived of its ability to block NDV–GFP replication (Fig. 3c, lane/panel 3). Once the neutralizing antibody had been inactivated by three cycles of freezing and thawing, the neutralization effect dissipated accordingly, as shown by the inhibition of viral GFP expression in Vero cells (Fig. 3c, lane/panel 2). In conclusion, our results revealed that it is IFN-β induced by NDV that exerts the main antiviral effect in the protective antiviral response.

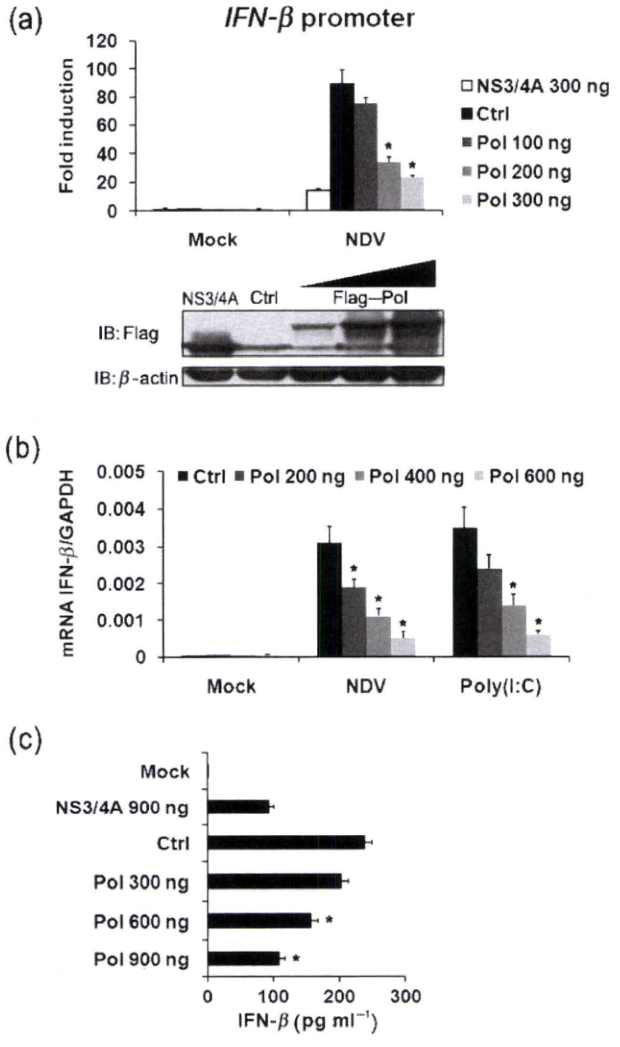


**Fig. 2.** HBV polymerase inhibits RIG-I- and TLR3-induced IFN-β promoter activity, transcription and expression in a dose-dependent manner. (a) PH5CH8 cells in 48-well plate were co-transfected with pIFN-β-Luc, pRL-TK and the indicated amounts of HBV polymerase (Pol) or NS3/4A. After 36 h, all of the cells were infected with 100 HAU NDV $ml^{-1}$ for 12 h and then harvested for luciferase activity (upper panel). The expression level of HBV polymerase was determined by immunoblotting (IB) using anti-Flag antibody (lower panel). (b) PH5CH8 cells in 24-well plates were transfected with increasing amounts of HBV polymerase. After 36 h, the cells were infected with 100 HAU NDV $ml^{-1}$ or treated with 50 μg poly(I:C) $ml^{-1}$ for an additional 6 h before measurement of *IFN-β* mRNA by real-time RT-PCR. (c) The amount of IFN-β produced by PH5CH8 cells in 12-well plates transfected with the indicated plasmids was determined by ELISA. *, $P<0.05$.

## HBV polymerase inhibits induction of IFN-β at the TBK1/IKKε level

The RLH and TLR signalling cascades that elicit *IFN-β* gene induction involve sensors, adaptors, kinases and transcriptional factors. To uncover the level at which HBV

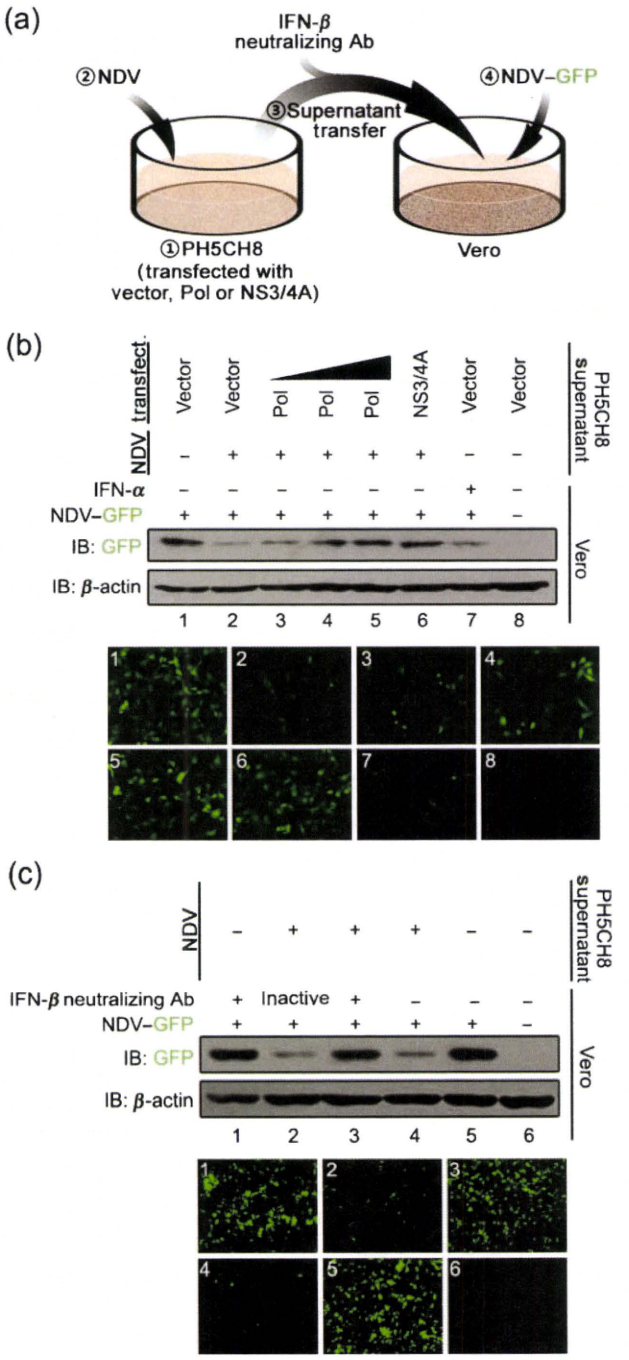


**Fig. 3.** HBV polymerase impairs cellular IFN-β-dependent antiviral immunity. (a) Scheme outlining the infection protection assay. The detailed protocol is described in Methods. (b) Vero cells were pre-treated with supernatant from NDV-treated PH5CH8 cells transfected with empty vector, Flag–Pol (Pol) or NS3/4A or with IFN-α (100 IU $ml^{-1}$) for 12 h, and then infected with NDV–GFP overnight. (c) Active or inactive IFN-β neutralizing antibody (10 μg $ml^{-1}$) was mixed with the supernatant from NDV-treated PH5CH8 cells and added to Vero cells for 12 h. The cells were then infected with NDV–GFP overnight. The GFP expression levels in (b) and (c) were examined by immunoblotting (IB) and microscopy.

polymerase interferes with IFN-$\beta$ induction, 293T cells were co-transfected with constructs of key regulatory molecules on the IFN-$\beta$ induction axis and HBV polymerase. Expression of RIG-I, ΔRIG-I, TRIF, IPS-1, TBK1, IKK$\varepsilon$ and an IRF3 dominant-positive mutant (IRF3-5D) in 293T cells enhanced *IFN-$\beta$* promoter activity (Fig. 4a–g). As a positive control, expression of HCV NS3/4A, which can cleave IPS-1 and TRIF (Li *et al.*, 2005b, c; Meylan *et al.*, 2005), blocked *IFN-$\beta$* promoter activity triggered by RIG-I, ΔRIG-I, TRIF and IPS-1 (Fig. 4a–d), but not TBK1, IKK$\varepsilon$ or IRF3-5D (Fig. 4e–g). However, in the presence of HBV polymerase, inhibition of *IFN-$\beta$* promoter activity was observed for all effectors tested except IRF3-5D (Fig. 4a–g). To confirm this observation, HEK293 cells were co-transfected with TBK1, IKK$\varepsilon$ or IRF3-5D and the indicated amounts of HBV polymerase. As expected, HBV polymerase inhibited *IFN-$\beta$* promoter activity triggered by TBK1 and IKK$\varepsilon$ in a dose-dependent manner (Fig. 4h), whilst it had no effect on activation by IRF3-5D, even at the highest HBV polymerase expression level (Fig. 4i). These results suggested that HBV polymerase inhibits IFN-$\beta$ induction at the level of TBK1/IKK$\varepsilon$.

## HBV polymerase inhibits IRF3 phosphorylation, dimerization and nuclear translocation

IRF3, a key transcriptional factor in IFN-$\beta$ induction, is regulated through phosphorylation by the TBK1 and IKK$\varepsilon$ kinases. Upon phosphorylation, IRF3 dimerizes and translocates into the nucleus, ultimately driving *IFN-$\beta$* transcription (Hiscott, 2007). In light of our results indicating that HBV polymerase inhibited IFN-$\beta$ induction at the level of TBK1/IKK$\varepsilon$, we further studied the phosphorylation, dimerization and nuclear translocation of IRF3 in the presence of HBV polymerase.

To examine the effect of HBV polymerase on IRF3 phosphorylation, PH5CH8 cells transfected with the indicated amounts of HBV polymerase were challenged with SeV infection. The results showed that IRF3 phosphorylation was inhibited with increasing HBV polymerase expression (Fig. 5a). Likewise, the effect of HBV polymerase on IRF3 dimerization was studied by native gel electrophoresis. As expected, SeV infection induced dimerization of IRF3 in the absence of HBV polymerase (Fig. 5b, lanes 2 and 4). In contrast, a dose-dependent reduction in dimerized IRF3 was observed in the presence of the polymerase (Fig. 5b, lanes 5–7). Next, we examined the subcellular localization of endogenous IRF3 with or without HBV polymerase expression. Immunofluorescence observations showed that, compared with empty vector control, IRF3 nuclear translocation was significantly reduced in response to SeV stimulation in PH5CH8 cells expressing HBV polymerase (Fig. 5c, and Supplementary Fig. S1a, available in JGV Online). This indicated that HBV polymerase inhibits IRF3 nuclear translocation. Similar results were also obtained in SeV-infected HepG2 cells co-transfected with trace amounts of RIG-I as well as wild-type HBV or HBV-ΔPol (Fig. 5d).

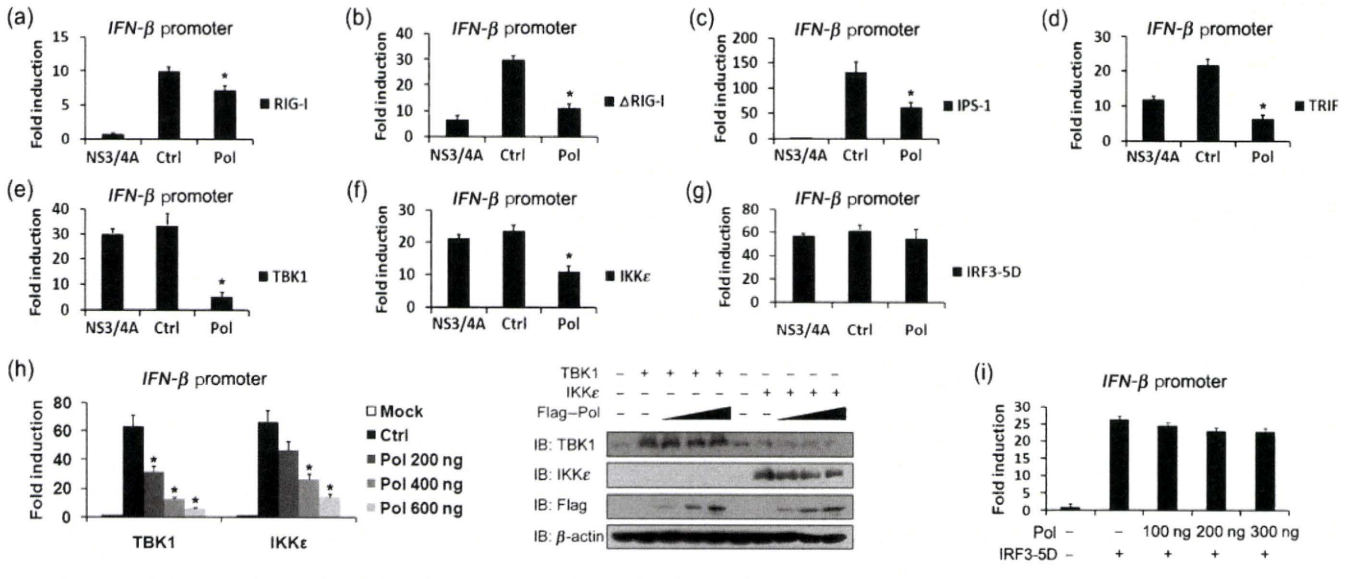


**Fig. 4.** HBV polymerase inhibits IFN-$\beta$ induction at the TBK1/IKK$\varepsilon$ level. 293T cells in 48-well plates were co-transfected with pIFN-$\beta$-Luc, pRL-TK and Flag–Pol (Pol) (200 ng) or NS3/4A (200 ng) along with 50 ng of expression plasmids encoding RIG-I (a), ΔRIG-I (b), IPS-1 (c), TRIF (d), TBK1 (e), IKK$\varepsilon$ (f) or IRF3-5D (g). After 36 h, the cells were harvested for luciferase activity. (h) HEK293 cells in 24-well plates were co-transfected with TBK1/IKK$\varepsilon$ together with the indicated amounts of Flag–Pol. After 36 h, the cells were harvested for luciferase activity (left panel). Expression of the indicated proteins was determined by immunoblotting (IB; right panel). (i) HEK293 cells in 48-well plate were co-transfected with IRF3-5D together with the indicated amounts of Flag–Pol. After 36 h, the cells were harvested for luciferase activity.

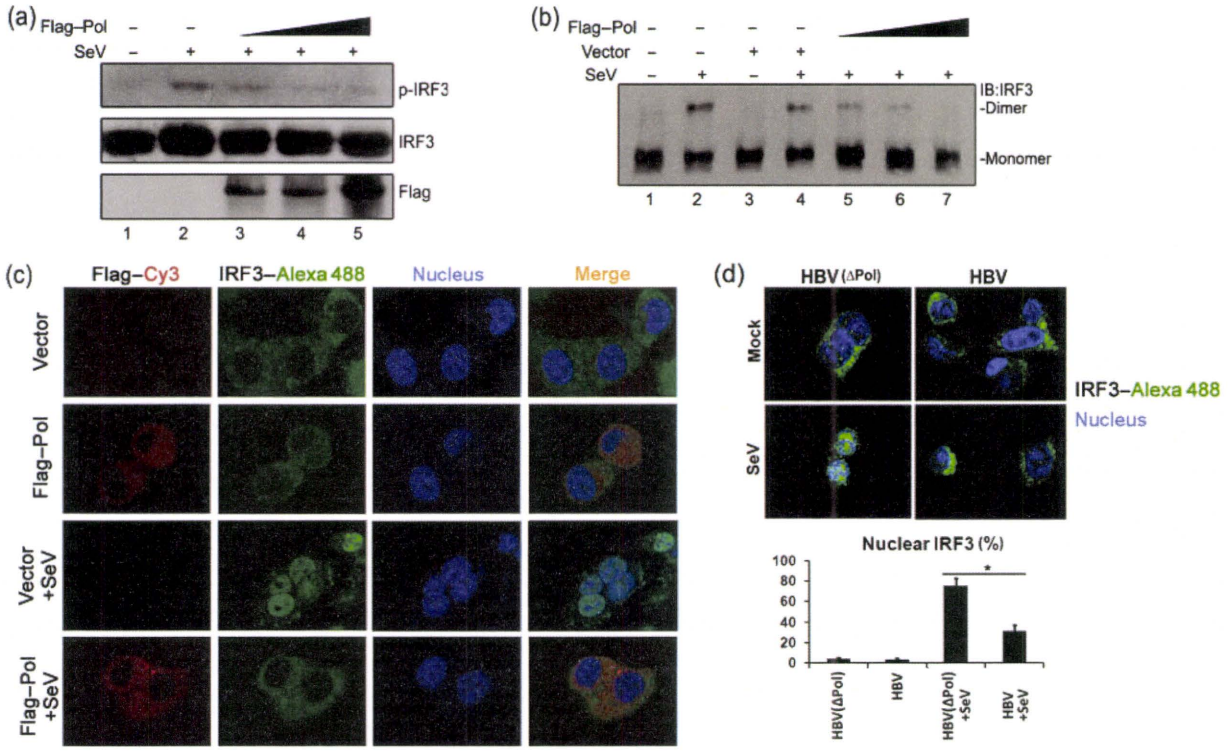


**Fig. 5.** HBV polymerase impedes IRF3 activation. (a, b) PH5CH8 cells in 12-well plates were transfected with increasing amounts of pQCXIP-3×Flag-Pol. After 24 h, the cells were selected with puromycin (3 μg ml$^{-1}$) for an additional 24 h and then infected with SeV (100 HAU ml$^{-1}$) for 6 h. Immunoblotting and native PAGE were performed to detect the phosphorylation (a) and dimerization (b) of IRF3. p-IRF3, phosphorylated IRF3. (c) Puromycin-selected cells were seeded onto chambered coverglass and challenged with or without SeV for an IRF3 nuclear translocation assay by immunofluorescence. (d) HepG2 cells were transfected with 5 ng RIG-I and 200 ng pQCXIP empty vector as well as 800 ng pHBV1.3 or HBV-ΔPol. After 24 h, the cells were transferred to chambered coverglass for puromycin selection for an additional 24 h, treated with or without SeV (100 HAU ml$^{-1}$) for 6 h and analysed for immunofluorescence using TO-PRO-3 and anti-IRF3 antibody (upper panel). The percentage of cells with nuclear IRF-3 from six independent experiments was calculated (mean ± SD) (lower panel).

However, no co-localization between HBV polymerase and IRF3 was observed (Fig. 5c). To confirm this result, Flag-tagged HBV polymerase was pulled down to analyse its binding proteins using immunoprecipitation. HBV polymerase and DDX3, but not IRF3, were detected in the immunoprecipitation complex (see Supplementary Fig. S1b). Thus, these results indicated that HBV polymerase interferes with IRF3 activation and that this inhibitory effect may be indirect.

## DDX3 is involved in the inhibition of IFN-β induction by HBV polymerase

DDX3 has been reported to be involved in TBK1/IKKε-mediated IRF activation and type I IFN induction (Schröder *et al.*, 2008; Soulat *et al.*, 2008). Moreover, DDX3 has been isolated from a Flag-tagged HBV polymerase immunoprecipitation complex using an anti-Flag pull-down assay (Wang *et al.*, 2009). Based on these studies, we speculated that DDX3 may also be involved in the inhibition of IFN-β induction by HBV polymerase. We first confirmed the involvement of endogenous DDX3 in IFN-β induction in our system using a DDX3 antisense construct (DDX3-AS) (Fig. 6a), and detected the co-localization of HBV polymerase and DDX3 in the cytoplasm (see Supplementary Fig. S2a, available in JGV Online). Next, we analysed the interaction between TBK1/IKKε and DDX3 in the presence of HBV polymerase. The amount of TBK1/IKKε was compared in the absence or presence of HBV polymerase. Consistent with previous reports (Schröder *et al.*, 2008; Soulat *et al.*, 2008; Wang *et al.*, 2009), TBK1/IKKε and HBV polymerase were detected in the DDX3 immunoprecipitation complex. However, less TBK1/IKKε was detected in the presence of HBV polymerase when compared with the absence of HBV polymerase (Fig. 6b and Supplementary Fig. S2b), suggesting that HBV polymerase can dampen the interaction between TBK1/IKKε and DDX3 through competitive binding of DDX3. Furthermore, HBV polymerase also inhibited the phosphorylation of DDX3 by TBK1/IKKε (Fig. 6c and Supplementary Fig. S2c). Finally, we examined whether overexpression of DDX3 could restore the inhibitory effect of HBV polymerase. As

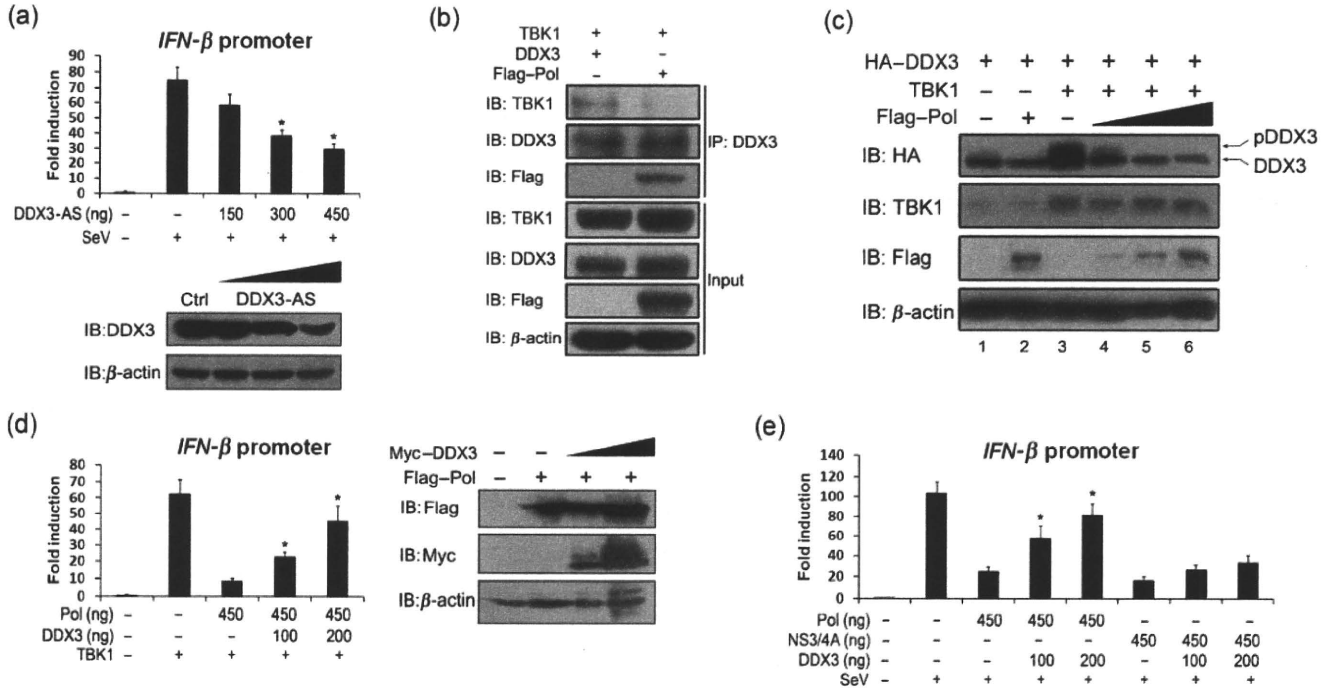


**Fig. 6.** DDX3 is involved in the inhibition of IFN-$\beta$ induction by HBV polymerase. (a) PH5CH8 cells in 24-well plates were transfected with pIFN-$\beta$-Luc, pRL-TK and the indicated amounts of DDX3-AS. After 48 h, cells were treated with 100 HAU SeV ml$^{-1}$ for 12 h before the luciferase activity assay (upper panel) and evaluation of DDX3-AS-mediated silencing of DDX3 by immunoblotting (IB; lower panel). (b) 293T cells in a 10 cm diameter dish were co-transfected with 5 μg TBK1, DDX3, Flag–Pol or empty vector. Cells were harvested for immunoprecipitation and immunoblotting at 48 h post-transfection. (c) HEK293 cells in 12-well plates were co-transfected with the indicated expression constructs. Cells were harvested for immunoblotting using the indicated antibodies at 48 h post-transfection. (d) 293T cells in 24-well plates were co-transfected with pIFN-$\beta$-Luc, pRL-TK, TBK1 and Flag–Pol as well as the indicated amounts of DDX3. After 36 h, the cells were harvested for luciferase activity (left panel). The expression of Myc–DDX3 and Flag–Pol were confirmed by immunoblotting (right panel). (e) PH5CH8 cells in 24-well plates were co-transfected with pIFN-$\beta$-Luc, pRL-TK and Flag–Pol or NS3/4A as well as the indicated amounts of DDX3. After 36 h, the cells were treated with 100 HAU SeV ml$^{-1}$ for 12 h and subjected to a luciferase assay.

expected, HBV polymerase-mediated inhibition of TBK1- and SeV-induced *IFN-β* promoter activation was rescued by DDX3 in a dose-dependent manner (Fig. 6d, e). However, HCV NS3/4A inhibition of IFN-$\beta$ promoter was not reversed by overexpression of DDX3 (Fig. 6e), which suggests that DDX3 interaction is at the heart of HBV polymerase inhibitory effects. All these results indicated that DDX3 is involved in the inhibition of IFN-$\beta$ induction by HBV polymerase.

## DISCUSSION

IFN-$\beta$ induction is one of the first-phase characteristics of activation of the type I IFN system. TLRs and RLHs, as molecular sensors to viral products, can trigger downstream adaptor aggregation and subsequent activation of TBK1/IKK$\varepsilon$, which ultimately phosphorylate IRF3. IRF3, together with other related transcription factors, can drive IFN-$\beta$ production in a concerted manner (Taniguchi & Takaoka, 2002). To evade recognition and the immune response, viruses have sophisticatedly generated viral partners to target the critical molecules in the IFN-$\beta$ induction pathway and have them hijacked or degraded, resulting in a relatively favourable environment for viral proliferation (Roy & Mocarski, 2007). For example, HCV NS3/4A can cleave TRIF and IPS-1 and consequently lead to acquired deficiency of IFN-$\beta$ induction in infected cells (Li *et al.*, 2005b, c; Meylan *et al.*, 2005). Ebola virus VP35, a component of the viral RNA polymerase complex, can also subvert host type I IFN induction via suppression of IRF3 activation (Basler *et al.*, 2003; Cardenas *et al.*, 2006). Here, we found that HBV polymerase could disturb RIG-I- and TLR3-mediated IFN-$\beta$ induction (Figs 1–3). Unlike HCV NS3/4A, the action target of HBV polymerase was defined at the TBK1/IKK$\varepsilon$ level (Fig. 4). Although HBV polymerase inhibited endogenous IRF3 activation (Fig. 5), a physical interaction was not detected (Supplementary Fig. S1b), which suggests that other molecular mechanisms underlie the inhibitory effect on IFN-$\beta$ induction.

Recent studies have identified DDX3 as another crucial molecule in TBK1/IKKε-mediated activation of IRFs and IFN-β synthesis (Schröder *et al.*, 2008; Soulat *et al.*, 2008). In addition, DDX3 also interacts with HBV polymerase and impedes viral reverse transcription by incorporation into nucleocapsids (Wang *et al.*, 2009). In this study, as no physical interaction was detected between IRF3 and HBV polymerase (Supplementary Fig. S1b), we speculated that DDX3 might be a candidate target for HBV inhibition of IFN-β induction at the TBK1/IKKε level. We found that HBV polymerase could dampen the interplay between TBK1/IKKε and DDX3 via competitive interaction (Fig. 6b and Supplementary Fig. S2b) and consequently impede DDX3 phosphorylation (Fig. 6c and Supplementary Fig. S2c). Furthermore, overexpression of DDX3 could rescue *IFN-β* promoter activity suppressed by HBV polymerase (Fig. 6d, e). This suggests that HBV polymerase can hijack endogenous DDX3 and subsequently dampen the interaction between TBK1/IKKε and DDX3 and ultimately inhibit IFN-β induction. This mechanism is similar to that of the vaccinia virus K7 protein (Kalverda *et al.*, 2009; Schröder *et al.*, 2008). Moreover, as the effect of HBV polymerase on TBK1 was more significant than on IKKε (Fig. 4h), we speculated that the difference in the effect of HBV polymerase on the two isozymes (TBK1 and IKKε) could be associated with the different affinity of the two kinases for DDX3. Interestingly, DDX3 ATPase activity is required for the inhibition of HBV replication but not for IRF activation and type I IFN induction (Schröder *et al.*, 2008; Soulat *et al.*, 2008; Wang *et al.*, 2009). Comprehensive analysis of the two sides of the interaction between DDX3 and HBV polymerase may shed light on the role of DDX3 in host cells against HBV infection. On the one hand, HBV might eliminate IFN-β induction via HBV polymerase hijacking of DDX3. On the other hand, host cells could still impede viral genome replication through impregnation of DDX3 into viral nucleocapsids even if IFN-β induction is blocked, which would partially explain the sophisticated strategy of host cells to suppress HBV replication. In addition, according to previous studies, no direct interaction has been observed between DDX3 and IRF3 (Schröder, 2010; Soulat *et al.*, 2008), and it is thus interesting to study whether and how DDX3 can impact on TBK1/IKKε activity and consequently affect the activation of IRF3. One hypothesis is that DDX3, as well as being one of the substrates of TBK1/IKKε, may also function as a scaffold protein like TANK protein to facilitate TBK1/IKKε activation.

The final outcome of virus infection depends on the balance of host response and virus countermeasures. However, the host immune response, including innate immunity and adaptive immunity, is contingent on the host recognition of invading viruses. HCV, a hepatotropic RNA virus, has been reported to trigger a hepatic innate immune response through the RIG-I signalling pathway (Saito *et al.*, 2008). Unlike HCV, it remains controversial whether HBV, a hepatotropic DNA virus, can be recognized by host cells in HBV infection (Lucifora *et al.*, 2010; Wieland & Chisari, 2005). Our study here demonstrated that HBV polymerase can inhibit IFN-β induction by RIG-I or TLR3 signal. Similarly, 2fTGH cells stably expressing the terminal protein domain of HBV polymerase have no response to dsRNA (Foster *et al.*, 1991). Moreover, HBsAg, HBeAg and even virion particles can also suppress TLR-mediated innate immunity and cytokine induction in primary hepatocytes (Wu *et al.*, 2009). All these findings provide evidence that HBV has developed strategies to subvert the host innate immune system; however, they also imply that HBV has the possibility of being recognized by host cells. There may be some leakage of viral DNA or RNA into the cytoplasm, either during entry of HBV into the cells or during exportation of viral RNA to the cytoplasm, which is then recognized by potential DNA or RNA sensors. It is worth noting that DNA viruses can be recognized through cellular RNA polymerase III coupled with the RIG-I pathway (Ablasser *et al.*, 2009; Chiu *et al.*, 2009). Therefore, to comprehensively elucidate the interaction between HBV and host innate immunity, both the recognition of HBV by the host immune system and how viral nucleic acids and proteins including HBV polymerase participate in the active evasion of recognition are worthy of further investigation.

In conclusion, our findings suggest a novel role of HBV polymerase in the inhibition of IFN-β induction in human hepatocytes. Further investigations will be conducted to confirm this novel function in stable cell lines and clinical samples, which will open up an exciting future for improving IFN treatment by triggering the pathway or molecules targeted by HBV.

## METHODS

**Cell culture.** PH5CH8 (a gift from Nobuyuki Kato, Okayama University Graduate School of Medicine and Dentistry, Japan), a simian virus 40 large T antigen-immortalized non-neoplastic human hepatocyte cell line with intact capacity for type I IFN induction (Li *et al.*, 2005a), was maintained as described previously (Noguchi & Hirohashi, 1996). HEK293, 293T, HepG2 and Vero cells (obtained from the Cell Bank of the Chinese Academy of Science) were cultured in Dulbecco's modified Eagle's medium supplemented with 10 % fetal bovine serum (FBS), penicillin (100 IU $ml^{-1}$; Gibco) and streptomycin (100 μg $ml^{-1}$; Gibco), in a 5 % $CO_2$ atmosphere at 37 °C.

**Plasmids and transfection.** The following expression plasmids were generously provided: pIFN-β-Luc (Dr Rongtuan Lin, McGill University, Canada); TBK1 and IKKε (Dr Katherine A. Fitzgerald, University of Massachusetts Medical School, MA, USA); TRIF, IRF3–GFP and IRF3-5D (Professor John Hiscott, McGill University); haemagglutinin (HA)–DDX3 and Myc–DDX3 (Professor Andrew G. Bowie, Trinity College Dublin, Ireland); RIG-I and IPS-1 (Takashi Fujita, Kyoto University, Japan); ΔRIG-I was amplified from RIG-I and cloned into a modified pcDNA3.1 vector containing three tandem Flag epitopes in frame at the 5′ end of the cloning site; HCV NS3/4A was amplified from cDNA of HCV replicon cells and cloned into the pcDNA3.1 vector by Dr Zhigang Yi (Fudan University, PR China); DDX3-AS (Kuan-Teh Jeang, National Institutes of Allergy and Infectious Diseases, MD, USA); HBV-ΔPol (Professor Jianming

Hu, The Pennsylvania State University, PA, USA) is a vector containing whole HBV genome with a point mutation changing the polymerase AUG to ACG making it deficient for polymerase synthesis while keeping the core protein unaltered; myc–p53 (Professor Jianxin Gu, Fudan University, PR China); pp53–Luc (Professor Lan Ma, Fudan University), Flag–Pol (pcDNA3.1-3 × Flag-Pol and pQCXIP-3 × Flag-Pol), pHBV1.3 (Professor Yumei Wen, Fudan University). HBV-Core and HBV-X were amplified from EGFP–Core and EGFP–X (Wu *et al.*, 2007), respectively, and cloned into pcDNA3.1-3 × Flag to make pcDNA3.1-3 × Flag-Core and pcDNA3.1-3 × Flag-HBx. All of the plasmids were sequenced and the indicated protein expression was confirmed by immunoblotting. PH5CH8, HEK293, 293T and HepG2 cells were transfected with the indicated plasmids using Fugene HD (Roche) or Lipofectamine 2000 (Invitrogen), according to the manufacturers' instructions.

**Poly(I:C), NDV, NDV–GFP and SeV.** Poly(I:C) was purchased from Sigma. NDV, NDV–GFP (a gift from Dr Yan Yuan, University of Pennsylvania, PA, USA) and SeV were propagated and purified from specific-pathogen-free-maintained chicken eggs. PH5CH8 cells were treated with 50 μg poly(I:C) $ml^{-1}$ added into the culture medium or infected with 100 haemagglutinin units (HAU) $ml^{-1}$ of the indicated virus and harvested 6 h later for RNA extraction or 12 h later for the luciferase reporter assay.

**Dual-luciferase reporter assay.** Cells ($3 \times 10^4$ per well) were seeded in a 48-well plate for culture overnight. The cells were then transfected with 20 ng pIFN-β-Luc, 5 ng pRL-TK (expressing *Renilla* luciferase; Promega) and the indicated amounts of expression plasmids. After 36 h, cells were mock treated or treated with poly(I:C), NDV or SeV for an additional 12 h. All cells were lysed with passive lysis buffer and assayed for luciferase activity with a Dual-Luciferase Assay kit (Promega). Firefly luciferase activities were normalized based on *Renilla* luciferase activities. The fold induction of promoter activity was calculated by dividing the normalized luciferase activity of stimulated cells by that of mock-treated cells. All reporter assays were repeated at least three times. The data shown are mean values ± SD from one representative experiment.

**Real-time RT-PCR.** Total cellular RNA was extracted with TRIzol reagent (Invitrogen), treated with DNase I (Takara) to remove genomic DNA contamination and reverse-transcribed using Toyobo Ace reverse transcriptase. The cDNA samples were subjected to real-time PCR using primers specific for IFN-β and glyceraldehyde 3-phosphate dehydrogenase (GAPDH): IFN-β forward, 5′-GATTCATCTAGCACTGGCTGG-3′, and reverse, 5′-CTTCAGGTAATGCAGAATCC-3′; GAPDH forward, 5′-GGTATCGTGGAAGGACTCATGA-3′, and reverse, 5′-ATGCCAGTGGCTTCCCGTTCAGC-3′. For comparisons, transcription of IFN-β was normalized to that of GAPDH.

**IFN-β ELISA.** The level of IFN-β in the culture medium was measured using an ELISA kit for human IFN-β (USCN Life Science) according to the manufacturer's instructions.

**Immunofluorescence.** PH5CH8 cells or HepG2 cells transfected with the indicated plasmids were seeded into a chambered coverglass system (Lab-Tek) for 24 h puromycin selection. Six hours after being treated with or without SeV, cells were fixed in 4% paraformaldehyde, permeabilized by the addition of 0.1% Triton X-100 and blocked with 10% FBS for 2 h. IRF3 was detected by staining with rabbit anti-human IRF3 (1:300 dilution; Santa Cruz Biotechnology), followed by Alexa 488-coupled goat anti-rabbit IgG (1:1000; Jackson Immunologicals). Flag-tagged HBV polymerase was detected by staining with anti-Flag antibody (1:2000; Sigma) followed by Cy3-coupled goat anti-mouse IgG (1:1000; Jackson Immunologicals), and the nuclei were counterstained with the DNA-specific stain TO-PRO-3 (1:1000; Invitrogen) or 4′-6-diamidino-2-phenylindole (DAPI, 1:1000; Invitrogen). The subcellular localization of IRF3 (green) and HBV polymerase (red) was observed with an Olympus FluoView FV1000 confocal microscope or Zeiss Axiovert 200 fluorescent microscope.

**Immunoprecipitation.** 293T or HepG2 cells were seeded into 10 cm dishes ($2 \times 10^6$ cells) and cultured overnight to 80–90% confluency before co-transfection with the indicated construct. Cells were harvested after 48 h in 1 ml lysis buffer [25 mM HEPES (pH 7.5), 100 mM NaCl, 1 mM EDTA, 10% glycerol, 0.2% NP-40 containing 1 × Roche protease inhibitors]. DDX3 polyclonal IgG was pre-coupled to Protein A/G PLUS–Agarose (Santa Cruz Biotechnology) for 1 h at 4 °C before incubation with the cell lysates for 4 h at 4 °C. The immune complexes were precipitated, washed and analysed by SDS-PAGE and immunoblotting.

**Immunoblotting.** Cellular extracts were subjected to immunoblotting analysis as described previously (Wu *et al.*, 2007). The antibodies used were as follows: mouse anti-Flag, mouse anti-Myc, mouse anti-β-actin (Sigma), rabbit anti-DDX3, rabbit anti-IRF3 (Santa Cruz Biotechnology), mouse anti-HA, rabbit anti-phospho-IRF3, rabbit anti-TBK1, rabbit anti-IKKε (Cell Signalling), and peroxidase-conjugated secondary goat anti-mouse and anti-rabbit antibodies (Amersham Biosciences). Protein bands were visualized using an ECL Plus Western blotting system (Perkin-Elmer) followed by exposure to Kodak Bio-Max film.

**Native PAGE.** The IRF3 dimerization assay was performed as described previously with a modification (Iwamura *et al.*, 2001). Briefly, $2 \times 10^5$ cells were seeded into a 12-well plate and cultured overnight. The PH5CH8 cells were transfected with the indicated amounts of HBV polymerase (empty vector was used to balance the total amount of DNA) using Fugene HD. After 24 h, cells were selected with puromycin (3 μg $ml^{-1}$) for 24 h and then infected with SeV or mock infected for an additional 6 h. The cells were harvested with 30 μl ice-cold lysis buffer [50 mM Tris/HCl, (pH 7.5), 150 mM NaCl and 0.5% NP-40 containing 1 × Roche protease inhibitors]. After centrifugation at 13 000 *g* for 10 min, supernatants were quantified using a BCA assay (Thermo Scientific) and diluted with 2 × native PAGE sample buffer [125 mM Tris/HCl (pH 6.8), 30% glycerol and 0.1% bromophenol blue], and then 20 μg of total protein was applied to a pre-run 7.5% native gel for separation. After electrophoresis, the gel was soaked in SDS electrophoresis buffer [25 mM Tris/HCl (pH 8.3), 250 mM glycine and 0.1% SDS] for 10 min at room temperature before the proteins were transferred onto a nitrocellulose membrane for immunoblotting.

**Infection protection assay.** PH5CH8 cells seeded in a 12-well plate and transfected with the indicated plasmids were challenged with NDV (100 HAU $ml^{-1}$) for 3 h and then rinsed five times with PBS and cultured for an additional 12 h. The culture medium was centrifuged for collection of the supernatants. Vero cells were pre-treated with these supernatants for 12 h and then infected with NDV–GFP (40 HAU $ml^{-1}$) overnight, followed by observation under a Zeiss Axiovert 200 fluorescent microscope and analysis by immunoblotting. The neutralization assay was performed by the addition of IFN-β neutralizing antibody (10 μg $ml^{-1}$; R&D Systems) into the supernatant.

**Statistical analysis.** All results were confirmed in at least three independent experiments in triplicate within each experiment. Data were analysed using Student's *t*-test and expressed as the mean ± SD. A value of $P<0.05$ was considered to be statistically significant.

## NOTE ADDED IN PROOF

Similar results to ours concerning the interaction with DDX3 were presented by other authors at the meeting on the Molecular Biology of Hepatitis B Viruses held in Tours, France, in September 2009 (Wang & Ryu, 2009), and have recently been accepted for publication (Wang & Ryu, 2010).

## ACKNOWLEDGEMENTS

We thank Nobuyuki Kato (Okayama University, Japan) for kindly providing PH5CH8 cells and Rongtuan Lin, John Hiscott (McGill University, Canada), Katherine Fitzgerald (University of Massachusetts Medical School, MA, USA), Takashi Fujita (Kyoto University, Japan), Kuan-Teh Jeang (National Institutes of Allergy and Infectious Diseases, MD, USA), Jianming Hu (The Pennsylvania State University, PA, USA), Yumei Wen, Jianxin Gu and Lan Ma (Fudan University, PR China) for their plasmids. We are grateful to Nathalie Grandvaux (University of Montreal, Canada) for immunoblotting advice. We are indebted to Professor Andrew Bowie and Dr Martina Schröder (Trinity College Dublin, Ireland) for Myc–DDX3 and helpful discussions. This work was financially supported by a Chinese State Basic Research Foundation Grant (2005CB522902), National High Tech Project (2006AA 02A411), National Megaprojects for Infectious Diseases (2008ZX10203) and the Program for Outstanding Medical Academic Leader of Shanghai to Z. Y. and a grant from the National Youth Foundation of China (no. 30900062) to M. W. J. C. was supported by a studentship from Shanghai Medical College.

## REFERENCES

**Ablasser, A., Bauernfeind, F., Hartmann, G., Latz, E., Fitzgerald, K. A. & Hornung, V. (2009).** RIG-I-dependent sensing of poly(dA:dT) through the induction of an RNA polymerase III-transcribed RNA intermediate. *Nat Immunol* **10**, 1065–1072.

**Basler, C. F., Mikulasova, A., Martinez-Sobrido, L., Paragas, J., Muhlberger, E., Bray, M., Klenk, H. D., Palese, P. & García-Sastre, A. (2003).** The Ebola virus VP35 protein inhibits activation of interferon regulatory factor 3. *J Virol* **77**, 7945–7956.

**Cardenas, W. B., Loo, Y. M., Gale, M., Jr, Hartman, A. L., Kimberlin, C. R., Martinez-Sobrido, L., Saphire, E. O. & Basler, C. F. (2006).** Ebola virus VP35 protein binds double-stranded RNA and inhibits alpha/beta interferon production induced by RIG-I signaling. *J Virol* **80**, 5168–5178.

**Chiu, Y. H., Macmillan, J. B. & Chen, Z. J. (2009).** RNA polymerase III detects cytosolic DNA and induces type I interferons through the RIG-I pathway. *Cell* **138**, 576–591.

**Crispe, I. N. (2009).** The liver as a lymphoid organ. *Annu Rev Immunol* **27**, 147–163.

**Ferreon, J. C., Ferreon, A. C., Li, K. & Lemon, S. M. (2005).** Molecular determinants of TRIF proteolysis mediated by the hepatitis C virus NS3/4A protease. *J Biol Chem* **280**, 20483–20492.

**Foster, G. R., Ackrill, A. M., Goldin, R. D., Kerr, I. M., Thomas, H. C. & Stark, G. R. (1991).** Expression of the terminal protein region of hepatitis B virus inhibits cellular responses to interferons alpha and gamma and double-stranded RNA. *Proc Natl Acad Sci U S A* **88**, 2888–2892.

**Ganem, D. & Prince, A. M. (2004).** Hepatitis B virus infection – natural history and clinical consequences. *N Engl J Med* **350**, 1118–1129.

**Hiscott, J. (2007).** Triggering the innate antiviral response through IRF-3 activation. *J Biol Chem* **282**, 15325–15329.

**Iwamura, T., Yoneyama, M., Yamaguchi, K., Suhara, W., Mori, W., Shiota, K., Okabe, Y., Namiki, H. & Fujita, T. (2001).** Induction of IRF-3/-7 kinase and NF-κB in response to double-stranded RNA and virus infection: common and unique pathways. *Genes Cells* **6**, 375–388.

**Kalverda, A. P., Thompson, G. S., Vogel, A., Schroder, M., Bowie, A. G., Khan, A. R. & Homans, S. W. (2009).** Poxvirus K7 protein adopts a Bcl-2 fold: biochemical mapping of its interactions with human DEAD box RNA helicase DDX3. *J Mol Biol* **385**, 843–853.

**Li, K., Chen, Z., Kato, N., Gale, M., Jr & Lemon, S. M. (2005a).** Distinct poly(I-C) and virus-activated signaling pathways leading to interferon-β production in hepatocytes. *J Biol Chem* **280**, 16739–16747.

**Li, K., Foy, E., Ferreon, J. C., Nakamura, M., Ferreon, A. C., Ikeda, M., Ray, S. C., Gale, M., Jr & Lemon, S. M. (2005b).** Immune evasion by hepatitis C virus NS3/4A protease-mediated cleavage of the Toll-like receptor 3 adaptor protein TRIF. *Proc Natl Acad Sci U S A* **102**, 2992–2997.

**Li, X. D., Sun, L., Seth, R. B., Pineda, G. & Chen, Z. J. (2005c).** Hepatitis C virus protease NS3/4A cleaves mitochondrial antiviral signaling protein off the mitochondria to evade innate immunity. *Proc Natl Acad Sci U S A* **102**, 17717–17722.

**Liaw, Y. F. & Chu, C. M. (2009).** Hepatitis B virus infection. *Lancet* **373**, 582–592.

**Lucifora, J., Durantel, D., Testoni, B., Hantz, O., Levrero, M. & Zoulim, F. (2010).** Control of hepatitis B virus replication by innate response of HepaRG cells. *Hepatology* **51**, 63–72.

**Meylan, E., Curran, J., Hofmann, K., Moradpour, D., Binder, M., Bartenschlager, R. & Tschopp, J. (2005).** Cardif is an adaptor protein in the RIG-I antiviral pathway and is targeted by hepatitis C virus. *Nature* **437**, 1167–1172.

**Noguchi, M. & Hirohashi, S. (1996).** Cell lines from non-neoplastic liver and hepatocellular carcinoma tissue from a single patient. *In Vitro Cell Dev Biol Anim* **32**, 135–137.

**Roy, C. R. & Mocarski, E. S. (2007).** Pathogen subversion of cell-intrinsic innate immunity. *Nat Immunol* **8**, 1179–1187.

**Saito, T., Owen, D. M., Jiang, F., Marcotrigiano, J. & Gale, M., Jr (2008).** Innate immunity induced by composition-dependent RIG-I recognition of hepatitis C virus RNA. *Nature* **454**, 523–527.

**Schröder, M. (2010).** Human DEAD-box protein 3 has multiple functions in gene regulation and cell cycle control and is a prime target for viral manipulation. *Biochem Pharmacol* **79**, 297–306.

**Schröder, M., Baran, M. & Bowie, A. G. (2008).** Viral targeting of DEAD box protein 3 reveals its role in TBK1/IKKε-mediated IRF activation. *EMBO J* **27**, 2147–2157.

**Seeger, C. & Mason, W. S. (2000).** Hepatitis B virus biology. *Microbiol Mol Biol Rev* **64**, 51–68.

**Soulat, D., Burckstummer, T., Westermayer, S., Goncalves, A., Bauch, A., Stefanovic, A., Hantschel, O., Bennett, K. L., Decker, T. & Superti-Furga, G. (2008).** The DEAD-box helicase DDX3X is a critical component of the TANK-binding kinase 1-dependent innate immune response. *EMBO J* **27**, 2135–2146.

**Takeuchi, O. & Akira, S. (2009).** Innate immunity to virus infection. *Immunol Rev* **227**, 75–86.

**Taniguchi, T. & Takaoka, A. (2002).** The interferon-$\alpha/\beta$ system in antiviral responses: a multimodal machinery of gene regulation by the IRF family of transcription factors. *Curr Opin Immunol* **14**, 111–116.

**van der Molen, R. G., Sprengers, D., Binda, R. S., de Jong, E. C., Niesters, H. G., Kusters, J. G., Kwekkeboom, J. & Janssen, H. L. (2004).** Functional impairment of myeloid and plasmacytoid dendritic cells of patients with chronic hepatitis B. *Hepatology* **40**, 738–746.

**Wang, H. & Ryu, W.-S. (2009).** HBV polymerase inhibits pattern recognition receptor-mediated innate immune response via its interaction with DDX3 DEAD-box RNA helicase. In *Abstracts of The Molecular Biology of Hepatitis B Viruses meeting*, Tours, 30 August–2 September 2009, p. 109. Doylestown, PA: Hepatitis B Foundation.

**Wang, H. & Ryu, W.-S. (2010).** Hepatitis B virus polymerase blocks pattern recognition receptor signaling via interaction with DDX3: implications for immune evasion. *PLoS Pathog* **6**, e1000986. doi:10.1371/journal.ppat.1000986

**Wang, H., Kim, S. & Ryu, W. S. (2009).** DDX3 DEAD-Box RNA helicase inhibits hepatitis B virus reverse transcription by incorporation into nucleocapsids. *J Virol* **83**, 5815–5824.

**Wieland, S. F. & Chisari, F. V. (2005).** Stealth and cunning: hepatitis B and hepatitis C viruses. *J Virol* **79**, 9369–9380.

**Wu, M., Xu, Y., Lin, S., Zhang, X., Xiang, L. & Yuan, Z. (2007).** Hepatitis B virus polymerase inhibits the interferon-inducible MyD88 promoter by blocking nuclear translocation of Stat1. *J Gen Virol* **88**, 3260–3269.

**Wu, J., Meng, Z., Jiang, M., Pei, R., Trippler, M., Broering, R., Bucchi, A., Sowa, J. P., Dittmer, U. & other authors (2009).** Hepatitis B virus suppresses Toll-like receptor-mediated innate immune responses in murine parenchymal and nonparenchymal liver cells. *Hepatology* **49**, 1132–1140.

Journal of Bioscience and Bioengineering
VOL. 110 No. 3, 374–376, 2010

www.elsevier.com/locate/jbiosc

TECHNICAL NOTE

# Generation of single-chain Fvs against detergent-solubilized recombinant antigens with a simple coating procedure

Torahiko Tanaka,[1,*] Yuichiro Hasegawa,[2,3] Makoto Saito,[2,3] Masanori Ikeda,[4] and Nobuyuki Kato[4]

*Department of Advanced Medical Science, Nihon University School of Medicine, 30-1 Oyaguchi-kamimachi, Itabashi, Tokyo 173-8610, Japan*[1]
*Department of Obstetrics and Gynecology, Nihon University School of Medicine, 30-1 Oyaguchi-kamimachi, Itabashi, Tokyo 173-8610, Japan*[2]
*Open Research Center for Genome and Infectious Disease Control, Nihon University School of Medicine, 30-1 Oyaguchi-kamimachi, Itabashi, Tokyo 173-8610, Japan*[3] *and Department of Tumor Virology, Okayama University Graduate School of Medicine, Dentistry, and Pharmaceutical Sciences, 2-5-1 Shikata-cho, Okayama 700-8558, Japan*[4]

Received 5 February 2010; accepted 29 March 2010

**Antigen coating on polystyrene is prevented by detergent. We present here a simple procedure to coat detergent-solubilized antigen for subsequent panning selection of single-chain Fv (scFv), the target antigen of which was the hepatitis C virus (HCV) non-structural protein (NS) 4B, an integral membrane protein.**



[**Key words:** Single-chain Fv; Detergent; Critical micelle concentration; Hepatitis C virus; NS4B]

The single-chain Fv (scFv)-phage display (1) is a useful technology to obtain antibodies against a wide category of antigens, including non-protein antigens, autoantigens, and antigens that are difficult to generate in animals. To obtain specific scFvs, panning selection has been performed on antigen-coated polystyrene using an scFv-phage display library (2). Antigen coating is achieved by the simple incubation of a soluble antigen solution in polystyrene tubes and wells. However, when an antigen is detergent-solubilized, detergent severely disturbs antigen coating on polystyrene (3,4) and this becomes an obstacle to the panning selection of scFv. To overcome the problem, we developed a simple procedure to coat an antigen by lowering the detergent concentration in an antigen solution with no additional material or time-consuming work. The target antigen was the hepatitis C virus (HCV) non-structural protein (NS) 4B, an integral membrane protein. HCV has a positive-stranded RNA genome encoding at least 10 viral proteins, namely, a core, E1, E2, p7, NS2, NS3, NS4A, NS4B, NS5A, and NS5B (5). The 5' untranslated region has a functional internal ribosome entry site, and the 3' untranslated region contains a highly conserved 98 nucleotide structure, the 3' X (6), which is indispensable for the viral genome replication. The NS proteins are thought to form complexes to replicate the viral genome. Little is known about the role of NS4B which harbors at least four transmembrane domains. Anti-NS4B scFvs to various epitopes are a useful tool for analyzing the roles of NS4B in virus replication.

We prepared the N-terminal hexahistidine (His)-tagged NS4B (NS4BHis) as an antigen based on the sequence of strain O (subtype 1b HCV) (7) using the pET expression system (Novagen, USA). The NS4B fragment was amplified by PCR using the restriction-site-tagged primers 5'-TTACATATGCATCACCACCATCACCATGGTGCCTCGCACC-TCCCTTAC-3' (with the *Nde*I site as underlined) and 5'-TTAGGATCCT-TAGCATGGCGTGGAGCAGTC-3' (with the *Bam*HI site as underlined) with a plasmid pON/C-5B/KE (7) as a template. The expression construct was created by ligating the *Nde*I–*Bam*HI-digested fragment of NS4B into the *Nde*I–*Bam*HI-digested pET3a vector. Similarly, the N-terminal Myc (EQKLISEEDL)-His-tagged NS4B (NS4BMycHis) construct was created by PCR using the primers 5'-TTACATATGGAACA-GAAACTGATTAGCGAAGAAGATCTGCATCACCACCATCACCATG-3' (with the *Nde*I site as underlined) and 5'-TTAGGATCCTTAGCATGGCGTGGAG-CAGTC-3' (with the *Bam*HI site as underlined) with the NS4BHis construct as the PCR template. NS4B proteins were expressed in *Escherichia coli* strain KRX (Promega, USA) in the presence of 0.1% rhamnose at 25 °C. The cells were suspended in a buffer containing 10 mM Tris–HCl, pH 7.4, 5 mM EDTA, and a Complete™ protease inhibitor cocktail (Roche, Germany), sonicated three times with 5 s bursts, and centrifuged at 5000*g* for 3 min. Because NS4BHis was recovered in the pellet, the solubilization conditions were examined. NS4BHis was efficiently solubilized in the presence of 0.5 M NaCl with 1% n-dodecyl β-D-maltoside (DDM) or Triton X-100 but not with Tween-20 and n-octyl β-D-glucoside (OG). After solubilization with DDM, NS4BHis was affinity-purified using Ni NTA agarose (Qiagen, USA) to near-homogeneity according to the manufacturer's protocol.

In the usual panning selection of antigen-specific scFv, the antigen is coated on polystyrene by simple incubation in an aqueous buffer. In the present work, the purified NS4BHis preparation contains 1% DDM, and, as described above, detergents are known to severely disturb antigen coating on polystyrene. Upon a preliminary experiment, we failed to efficiently coat NS4BHis with 50-fold simple dilution (final

* Corresponding author. Present address: Division of Biochemistry, Department of Biomedical Sciences, Nihon University School of Medicine, 30-1 Oyaguchi-kamimachi, Itabashi, Tokyo 173-8610, Japan. Tel.: +81 3 3972 8111x2241; fax: +81 3 3972 8199.
*E-mail address:* tanakat@med.nihon-u.ac.jp (T. Tanaka).

1389-1723/$ - see front matter © 2010, The Society for Biotechnology, Japan. All rights reserved.
doi:10.1016/j.jbiosc.2010.03.014

DDM, 0.02%) on polystyrene. We then modified the purification step to lower the DDM concentration. After NS4BHis was bound to Ni affinity resin, washing and elution were conducted using a buffer with a low but slightly higher than critical micelle concentration (CMC) of DDM (0.01%; the CMC of DDM is 0.0087%). In detail, the Ni affinity resin was pre-equilibrated with a TBS buffer (10 mM Tris–HCl, pH 7.4, 0.15 M NaCl) containing 0.01% DDM and 20 mM imidazole, and the solubilized NS4BHis sample (to which 20 mM imidazole was also added) was applied to the resin. The bound NS4BHis was washed first with a 10-bed volume of the same buffer for equilibration and then with a 10-bed volume of TBS-0.01% DDM-0.5 M NaCl-20 mM imidazole, pH 7.4. Finally, the bound NS4B was eluted with a three-bed volume of TBS-0.01% DDM-0.5 M NaCl-0.25 M imidazole, pH 7.4. Under these conditions, NS4BHis could be purified and concentrated efficiently. Interestingly, even with 0.005% DDM, NS4BHis was efficiently purified in a similar manner. By further 50-fold dilution with a detergent-free buffer (final DDM concentration, 0.0002%), the NS4BHis was found to be coated on polystyrene efficiently. Thus a simple coating protocol for detergent-solubilized antigens was established by a modification of purification procedure to lower detergent concentrations.

We examined the concentration limits of frequently used detergents, including DDM, which enable the coating of NS4BHis (Fig. 1). For this purpose, NS4BMycHis was prepared using the same purification protocol as for NS4BHis with 0.01% of DDM. The NS4BMycHis solution was incubated in polystyrene wells in a microtiter plate with or without various concentrations of detergent (NP40, Triton X-100, Tween-20, OG, and DDM). In this experiment, a 1 µl (2.5 µg) purified NS4BMycHis preparation containing 0.01% DDM was diluted to 50 µl with a TBS buffer for each well; thus, the coating solution contained 0.0002% of carry-over DDM. After 6 h of incubation, each well was blocked, and the amount of adsorbed NS4BMycHis was evaluated using an anti-myc antibody HRP conjugate and the peroxidase-dependent colorimetric

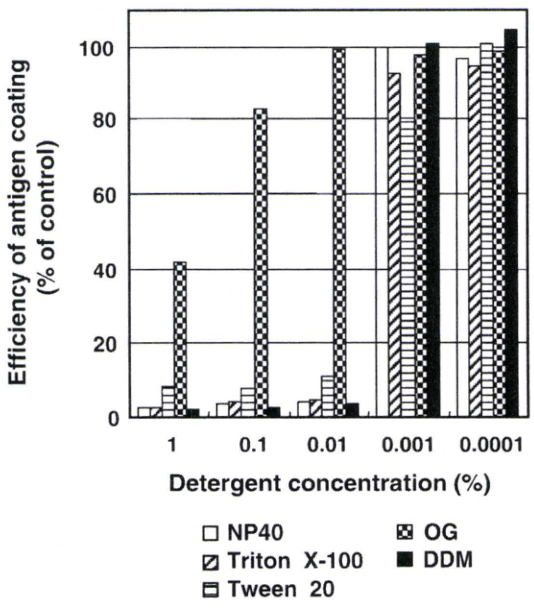


FIG. 1. The influence of various detergents on the coating of NS4B to microplate wells. All the reactions were carried out with final volume of 50 µl in microplate wells (Iwaki, Japan). NS4BMycHis (2.5 µg) was incubated for 6 h at room temperature in the absence or presence of an indicated concentration of detergent (NP 40, Triton X-100, Tween 20, OG, or DDM). The wells were washed 10 times with ultrapure water and blocked with a 5% skim milk-TBS buffer (MTBS) for 1 h. After washing, the wells were reacted with 200-fold diluted anti-myc antibody HRP conjugate (Wako Chemical, Japan) in 5% MTBS for 1 h. After washing, the wells were reacted with 2, 2'-azino-bis(3-ethylbenzthiazoline-6-sulfonic acid) (ABTS; Sigma, USA) according to manufacturer's protocol and the absorbance at 405 nm was determined. Data are the mean of two independent experiments and shown as a % of the control value obtained in the absence of detergent.

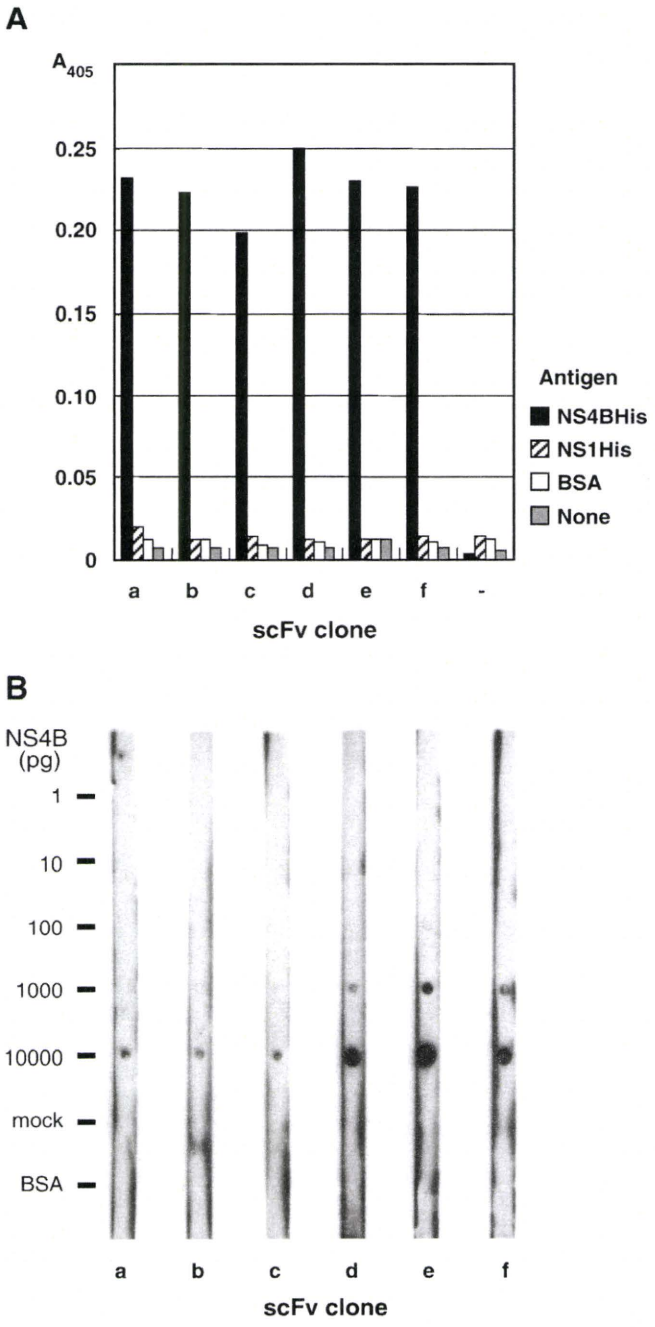


FIG. 2. Specificity and sensitivity assays of scFv phage clones against NS4B. (A) Confirmation of the antigen specificity by ELISA. All the reactions were carried out with final volume of 50 µl in each well. Indicated antigens (1 µg in TBS buffer); NS4BHis (containing 0.0002% DDM as final concentration), influenza virus NS1His (8), and bovine serum albumin (BSA) or TBS buffer alone (None), were incubated in wells of a microplate at 4 °C overnight. The wells were washed 10 times with ultrapure water and blocked with a 5% MTBS for 1 h. The wells were then incubated with or without (−) phage clones (a to f, $2.5 \times 10^9$ cfu in 5% MTBS) for 1 h, followed by incubation with 10,000-fold dilution of anti-M13 antibody HRP conjugate (GE, USA) in 5% MTBS for 30 min. Reaction was developed with ABTS and the absorbance at 405 nm was determined. (B) A sensitivity assay of scFv clones against NS4B. Indicated amounts of NS4BHis (0 [mock], 1, 10, 100, 1000, and 10,000 pg) and BSA (10 ng) in 0.5 µl TBS-0.01% DDM were spotted on nitrocellulose strips, air-dried, and incubated in TBS-0.1% Tween-20 overnight. After washing with ultrapure water, the spots were blocked, reacted with scFv phage ($5 \times 10^{10}$ cfu/ml in 5% MTBS) for 1 h, and visualized using an anti-M13 antibody HRP (horseradish peroxidase) conjugate and the ECL-Plus Western Blotting Detection Kit (GE Healthcare, UK) as described previously (9,11).

method. As shown in Fig. 1, the addition of 0.01% or more detergent, except for OG, severely disturbed the coating of NS4BMycHis, while that of 0.001% or lower detergent did not; only when 0.001% Tween-20 was used was the coating slightly disturbed. The results suggest that antigens cannot be coated on polystyrene in the presence of these detergents under concentrations usually used for solubilization (0.1–1.0%). On the other hand, about 80% of coating efficiency was achieved under 0.1% OG, suggesting that OG is convenient for solubilization of antigens to be coated on polystyrene as far as it efficiently solubilizes the target antigens (as described above, NS4B could not, unfortunately, be solubilized efficiently with OG). An antigen solution containing 1% OG would be coated efficiently by simple dilution.

Then we carried out the selection of scFvs against NS4B from a human naive scFv phage display library ($2.6\times10^9$ clones) (8) by usual panning protocol (2) with minor modifications. Polystyrene tubes (Maxisorp™, Nunc) were coated with NS4BHis (10 μg/ml in TBS buffer containing 0.0001% DDM as final concentration) and used for the selection. After blocking with 5% skim milk-TBS buffer (MTBS) for 1 h, the library phage ($1\times10^{12}$ cfu/ml of 5% MTBS) were incubated with the antigen for 1 h. After washing with TBS-0.1% Tween-20 for 10 times and then with TBS for 3 times, phage were eluted with 1.4% triethylamine and neutralized with a half volume of 1 M Tris–HCl pH 7.4. The phage were amplified in TG1 and used for the subsequent panning selection in the same manner. The reaction volume for antigen coating and phage reaction was 2 ml for the first round and 1 ml for the second and third round selections. After three rounds of selection, 6 independent clones (a to f) were obtained based on *Hae*III fingerprinting of the Fv region (9). Sequencing of the Fv region confirmed that these 6 clones were distinct (data not shown). The antigen specificity of the clones was confirmed by enzyme-linked immunosorbent assay (ELISA). As shown in Fig. 2A, all of the 6 clones reacted with NS4BHis but not with unrelated proteins such as bovine serum albumin (BSA) and unrelated His-tagged protein, influenza virus NS1His (8). The clones also did not react with uncoated wells. Thus the selected clones are specific to NS4B. To conveniently evaluate the sensitivity of selected scFvs, we spotted NS4BHis (1, 10, 100, 1000, 10,000 pg) and BSA (10 ng, as a negative control) on a nitrocellulose membrane and used it for dot blot analysis (Fig. 2B). Clones d, e, and f detected until the 1000 pg spot, and clones a, b, and c detected until the 10,000 pg spot. No clones detected the BSA spot. In our experience, scFv phages which can detect 100–10,000 pg of antigen spots were usually obtained by panning selection using a polystyrene-coated soluble antigen which was prepared without detergent. This suggests that the clones obtained in this work using a detergent-solubilized antigen were in a similar range of antigen affinity to clones against other soluble antigens obtained without detergent.

As described, the problem in the panning selection of scFv against detergent-solubilized antigens is more severe with low-CMC detergents, such as Triton X-100, as demonstrated by Gardas et al. (4), who found a strong correlation between the detergent CMC and the detergent concentration which inhibits protein binding to polystyrene. Presumably, the detergent micelle and protein molecule compete upon binding to polystyrene. This had also been suggested by Kenny et al. (10) when they showed that a higher molar ratio of antigen to detergent achieved a more efficient coating. The molecular structure and nature of detergents and proteins, such as hydrophobicity and hydrophilicity, may also affect which detergents and proteins have stronger affinities to polystyrene. In the present work, we found that the practical value of detergent concentration to enable efficient coating of a detergent-solubilized antigen is around 0.001% for frequently used low-CMC detergents, such as Triton X-100, Tween-20, NP40, and DDM. This value may also depend on the antigen concentration; we employed a relatively high antigen concentration (2.5 μg/50 μl = 50 μg/ml). Our procedure, in which the detergent concentration is lowered to a value near the CMC value during column work, is rapid and convenient to obtain a higher molar ratio of antigen to detergent. In this sense, our procedure is advantageous, especially when proteins are purified with affinity chromatography, since proteins are easily concentrated without an increase of the detergent concentration. Interestingly, even with the DDM concentration slightly lower than the CMC, recombinant NS4B was efficiently purified with Ni affinity chromatography. How low the detergent concentrations can be for target proteins to be efficiently purified may depend on the protein nature. Practically, researchers can easily evaluate whether a target protein can be purified well in detergent concentrations near CMC. In conclusion, if a target antigen can be solubilized by low-CMC detergent but not by high-CMC detergent, such as OG (CMC, 0.73%), as in the case of NS4B, our simple procedure is meaningful for the generation of scFv and other polystyrene-based work, such as the enzyme-linked immunosorbent assay and monoclonal antibody screening.

## ACKNOWLEDGMENTS

This work was supported by a Nihon University Joint Research Grant, a grant from the Ministry of Education, Culture, Sports, Science, and Technology to promote open research for young academics and specialists, and the grant "Strategic Research Base Development" Program for Private Universities subsidized by MEXT (2008). We thank Dr. T. Hayashida (Northwestern University) for suggestions.

## References

1. **Clackson, T., Hoogenboom, H. R., Griffiths, A. D., and Winter, G.:** Making antibody fragments using phage display libraries, Nature, **352**, 624–628 (1991).
2. **Griffiths, A. D., Williams, S. C., Hartley, O., Tomlinson, I. M., Waterhouse, P., Crosby, W. L., Kontermann, R. E., Jones, P. T., Low, N. M., and Allison, T. J., et al.:** Isolation of high affinity human antibodies directly from large synthetic repertoires, EMBO J., **13**, 3245–3260 (1994).
3. **Palfree, R. G. and Elliott, B. E.:** An enzyme-linked immunosorbent assay (ELISA) for detergent solubilized Ia glycoproteins using nitrocellulose membrane discs, J. Immunol. Methods, **52**, 395–408 (1982).
4. **Gardas, A. and Lewartowska, A.:** Coating of proteins to polystyrene ELISA plates in the presence of detergents, J. Immunol. Methods, **106**, 251–255 (1988).
5. **Kato, N.:** Molecular virology of hepatitis C virus, Acta Med. Okayama, **55**, 133–159 (2001).
6. **Tanaka, T., Kato, N., Cho, M. J., and Shimotohno, K.:** A novel sequence found at the 3' terminus of hepatitis C virus genome, Biochem. Biophys. Res. Commun., **215**, 744–749 (1995).
7. **Ikeda, M., Abe, K., Dansako, H., Nakamura, T., Naka, K., and Kato, N.:** Efficient replication of a full-length hepatitis C virus genome, strain O, in cell culture, and development of a luciferase reporter system, Biochem. Biophys. Res. Commun., **329**, 1350–1359 (2005).
8. **Murayama, R., Harada, Y., Shibata, T., Kuroda, K., Hayakawa, S., Shimizu, K., and Tanaka, T.:** Influenza A virus non-structural protein 1 (NS1) interacts with cellular multifunctional protein nucleolin during infection, Biochem. Biophys. Res. Commun., **362**, 880–885 (2007).
9. **Tanaka, T., Ito, T., Furuta, M., Eguchi, C., Toda, H., Wakabayashi-Takai, E., and Kaneko, K.:** In situ phage screening. A method for identification of subnanogram tissue components in situ, J. Biol. Chem., **277**, 30382–30387 (2002).
10. **Kenny, G. E. and Dunsmoor, C. L.:** Principles, problems, and strategies in the use of antigenic mixtures for the enzyme-linked immunosorbent assay, J. Clin. Microbiol., **17**, 655–665 (1983).
11. **Watanabe, N., Sasaoka, T., Noguchi, S., Nishino, I., and Tanaka, T.:** Cys669-Cys713 disulfide bridge formation is a key to dystroglycan cleavage and subunit association, Genes Cells, **12**, 75–88 (2007).

OPEN ACCESS Freely available online

PLoS one

# Hepatitis C Virus Core Protein Abrogates the DDX3 Function That Enhances IPS-1-Mediated IFN–Beta Induction

**Hiroyuki Oshiumi[1], Masanori Ikeda[2], Misako Matsumoto[1], Ayako Watanabe[1], Osamu Takeuchi[3], Shizuo Akira[3], Nobuyuki Kato[2], Kunitada Shimotohno[4], Tsukasa Seya[1]***

**1** Department of Microbiology and Immunology, Hokkaido University Graduate School of Medicine, Sapporo, Japan, **2** Department of Tumor Virology, Okayama University Graduate School of Medicine, Dentistry, and Pharmaceutical Sciences, Okayama, Japan, **3** Laboratory of Host Defense, WPI Immunology Frontier Research Center, Research Institute for Microbial Diseases, Osaka University, Suita, Japan, **4** Research Institute, Chiba Institute of Technology, Narashino, Japan

## Abstract

The DEAD box helicase DDX3 assembles IPS-1 (also called Cardif, MAVS, or VISA) in non-infected human cells where minimal amounts of the RIG-I-like receptor (RLR) protein are expressed. DDX3 C-terminal regions directly bind the IPS-1 CARD-like domain as well as the N-terminal hepatitis C virus (HCV) core protein. DDX3 physically binds viral RNA to form IPS-1-containing spots, that are visible by confocal microscopy. HCV polyU/UC induced IPS-1-mediated interferon (IFN)-beta promoter activation, which was augmented by co-transfected DDX3. DDX3 spots localized near the lipid droplets (LDs) where HCV particles were generated. Here, we report that HCV core protein interferes with DDX3-enhanced IPS-1 signaling in HEK293 cells and in hepatocyte Oc cells. Unlike the DEAD box helicases RIG-I and MDA5, DDX3 was constitutively expressed and colocalized with IPS-1 around mitochondria. In hepatocytes (O cells) with the HCV replicon, however, DDX3/IPS-1-enhanced IFN-beta-induction was largely abrogated even when DDX3 was co-expressed. DDX3 spots barely merged with IPS-1, and partly assembled in the HCV core protein located near the LD in O cells, though in some O cells IPS-1 was diminished or disseminated apart from mitochondria. Expression of DDX3 in replicon-negative or core-less replicon-positive cells failed to cause complex formation or LD association. HCV core protein and DDX3 partially colocalized only in replicon-expressing cells. Since the HCV core protein has been reported to promote HCV replication through binding to DDX3, the core protein appears to switch DDX3 from an IFN-inducing mode to an HCV-replication mode. The results enable us to conclude that HCV infection is promoted by modulating the dual function of DDX3.

**Citation:** Oshiumi H, Ikeda M, Matsumoto M, Watanabe A, Takeuchi O, et al. (2010) Hepatitis C Virus Core Protein Abrogates the DDX3 Function That Enhances IPS-1-Mediated IFN-Beta Induction. PLoS ONE 5(12): e14258. doi:10.1371/journal.pone.0014258

**Editor:** Jörn Coers, Duke University Medical Center, United States of America

**Received** May 28, 2010; **Accepted** November 16, 2010; **Published** December 8, 2010



**Funding:** This work was supported in part by the Program of Founding Research Centers for Emerging and Reemerging Infectious Diseases, MEXT, Sapporo Biocluster "Bio-S", the Knowledge Cluster Initiative of the MEXT, Grants-in-Aid from the Ministry of Education, Science, and Culture (Specified Project for Advanced Research) and the Ministry of Health, Labor, and Welfare of Japan, Mochida Foundation, Yakult Foundation, NorthTec Foundation and Waxman Foundation. The funders had no role in study design, data collection and analysis, decision to publish, or preparation of the manuscript.

**Competing Interests:** The authors have declared that no competing interests exist.

* E-mail: seya-tu@pop.med.hokudai.ac.jp

## Introduction

The retinoic acid inducible gene-I (RIG-I) and the melanoma differentiation-associated gene 5 (MDA5) encode cytoplasmic RNA helicases [1–3] that signal the presence of viral RNA through the adaptor, IPS-1/Mitochondrial antiviral signaling protein (MAVS)/Caspase recruitment domain (CARD) adaptor inducing interferon (IFN)-beta (Cardif)/Virus-induced signaling adaptor (VISA) to produce IFN-beta [4–7]. IPS-1 is localized to the mitochondrial outer membrane through its C-terminus [6]. Increasing evidence suggests that the DEAD-box RNA helicase DDX3, which is on the X chromosome, participates in the regulation of type I IFN induction by the RIG-I pathway.

DDX3 acts on the IFN-inducing pathway by a complex mechanism. Early studies reported that DDX3 up-regulates IFN-beta induction by interacting with IKKepsilon [8] or TBK1 [9] in a kinase complex. Both TBK1 and IKKepsilon are IRF-3-activating kinases with NF-kappaB- and IFN-inducible properties. DDX3 has been proposed to bind IKKepsilon, and IKKepsilon is generated after NF-kappaB activation [10]. Yeast two-hybrid studies demonstrated that DDX3 binds IPS-1, and both are constitutively present prior to infection (Fig. 1). Ultimately, DDX3 forms a complex with the DEAD-box RNA helicases RIG-I and MDA5 [11], which are present at only low amounts in resting cells, and are up-regulated during virus infection. Previously we used gene silencing and disruption, to show that the main function of DDX3 is to interact with viral RNA and enhance RIG-I signaling upstream of NAP1/TBK1/IKKepsilon [11]. Hence, DDX3 is involved in multiple pathways of RNA sensing and signaling during viral infection.

DDX3 resides in both the nucleus and the cytoplasm [12], and has been implicated in a variety of processes in gene expression regulation, including transcription, splicing, mRNA export, and translation [13]. A recent report suggested that the N-terminus of hepatitis C virus (HCV) core protein binds the C-terminus of DDX3 (Fig. S1) [14,15], and this interaction is required for HCV replication [16]. Although DDX3 promotes efficient HCV infection by accelerating HCV RNA replication, the processes

A

Two representative polyI:C-binding proteins identified by mass-spectrometric analysis

| dsRNA-binding protein | ID | Mr (kDa) | polyI:C | polyU | gene name |
|---|---|---|---|---|---|
| dsRNA-activated protein kinase | IPI00019463 | 63 kDa | 37 | 2 | PKR |
| ATP-dependent RNA helicase | IPI00215637 | 73 kDa | 19 | 12 | DDX3 |

B

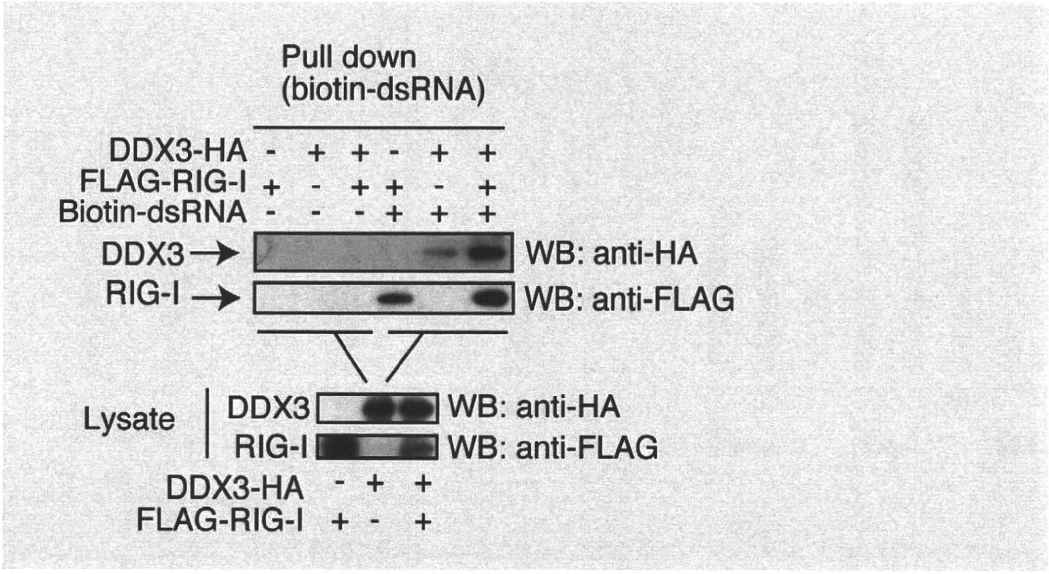


**Figure 1. DDX3 is a RNA-binding protein.** (A) DDX3 is a polyU- and polyI:C-binding protein. Mass spectrometry analyses indicated that DDX3 binds polyI:C- and polyU-Sepharose, although PKR binds polyI:C but not polyU. The rough data from MASCOT and one representative of six trials are shown. (B) DDX3 binds dsRNA, RIG-I and HCV core protein. Expression vectors for Flag-tagged RIG-I and HA-tagged DDX3 were transfected into HEK293 cells using lipofectamine 2000. Twenty-four hours after the transfection, extract from transfected cells were mixed with biotin-conjugated dsRNA. RNA-protein complex were recovered by pull-down assay using streptavidin-Sepharose. The protein within the pull-down fraction was analyzed by western blotting. The results are representative of two independent experiments.
doi:10.1371/journal.pone.0014258.g001

appear independent of its interaction with the viral core protein [15]. HCV seems to co-opt DDX3, and require DDX3 for replication. In addition, the association between DDX3 and core protein implicates DDX3 in HCV-related hepatocellular carcinoma progression [17]. Therefore, DDX3 could be a novel target for the development of drugs against HCV [18].

A number of reports have demonstrated the formation of the DDX3-core protein complex in the cytoplasm, but the functional relevance of DDX3-core protein interaction is not known. In this report, we show evidence that the HCV core protein participates in suppression of DDX3-augmented IPS-1 signaling for IFN-β induction. Several possible functions of DDX3 are discussed, focusing on its core protein association and IPS-1-regulatory properties.

## Materials and Methods

### Cell culture and reagents

HEK293 cells and HEK293FT cells were maintained in Dulbecco's Modified Eagle's low or high glucose medium (Invitrogen, Carlsbad, CA) supplemented with 10% heat-inactivated FCS (Invitrogen) and antibiotics. Huh7.5 cells were maintained in MEM (Nissui, Tokyo, Japan) supplemented with 10% heat-inactivated FCS. Hepatocyte sublines with HCV replicon (O cells) and without replicon (Oc cells) were established as described previously [19]. O cells with core-less subgenomic replicon (sO cells) were also generated in Dr. Kato's laboratory [16,19]. RIG-I −/− mouse embryonic fibroblasts (MEF) were gifts from Drs. Takeuchi and Akira [1]. Anti-FLAG M2 monoclonal Ab and anti-HA polyclonal Ab were purchased from Sigma. A mitochondria marker (Mitotracker) and Alexa Fluor®-conjugated secondary antibodies were purchased from Molecular probe. Anti-HCV core mAb (C7-50) [20] and anti-human DDX3 pAb were from Affinity BioReagents, Inc and Abcam, Cambridge MA, respectively.

### Plasmids

DDX3 cDNA encoding the entire ORF was cloned into pCR-blunt vector using primers, DDX3N F-Xh (CTC GAG CCA CCA TGA GTC ATG TGG CAG TGG AA) and DDX3C R-Ba (GGA TCC GTT ACC CCA CCA GTC AAC CCC) from human lung cDNA library. To make an expression plasmid, HA tag was fused at the C-terminal end of the full length DDX3 (pEF-BOS DDX3-HA). pEF-BOS DDX3 (1-224aa) vector was made by using primers,

DDX3 N-F-Xh and DDX3D1 (GGA TCC GGC ACA AGC CAT CAA GTC TCT TTT C). pEF-BOS DDX3-HA (225-662) was made by using primers, DDX3D2-3 (CTC GAG CCA CCA TGC AAA CAG GGT CTG GAA AAA C) and DDX3C R-Ba. To make pEF-BOS DDX3-HA (225-484) and pEF-BOS DDX3-HA (485-663), the primers, DDX3D2 R-Ba (GGA TCC AAG GGC CTC TTC TCT ATC CCT C) and DDX3D3 F-Xh (CTC GAG CCA CCA TGC ACC AGT TCC GCT CAG GAA AAA G) were used, respectively. HCV core expressing plasmids, pcDNA3.1 HCVO core or JFH1 core, were previously reported by N. Kato (Okayama University Japan) [16]. Another 1b genotype of the core was cloned from a HCV patient in Osaka Medical Center (Osaka) according to the recommendation of the Ethical Committee in Osaka. We obtained written informed consent from each patient for research use of their samples. Reporter and internal control plasmids for reporter gene assay are previously described [21,22].

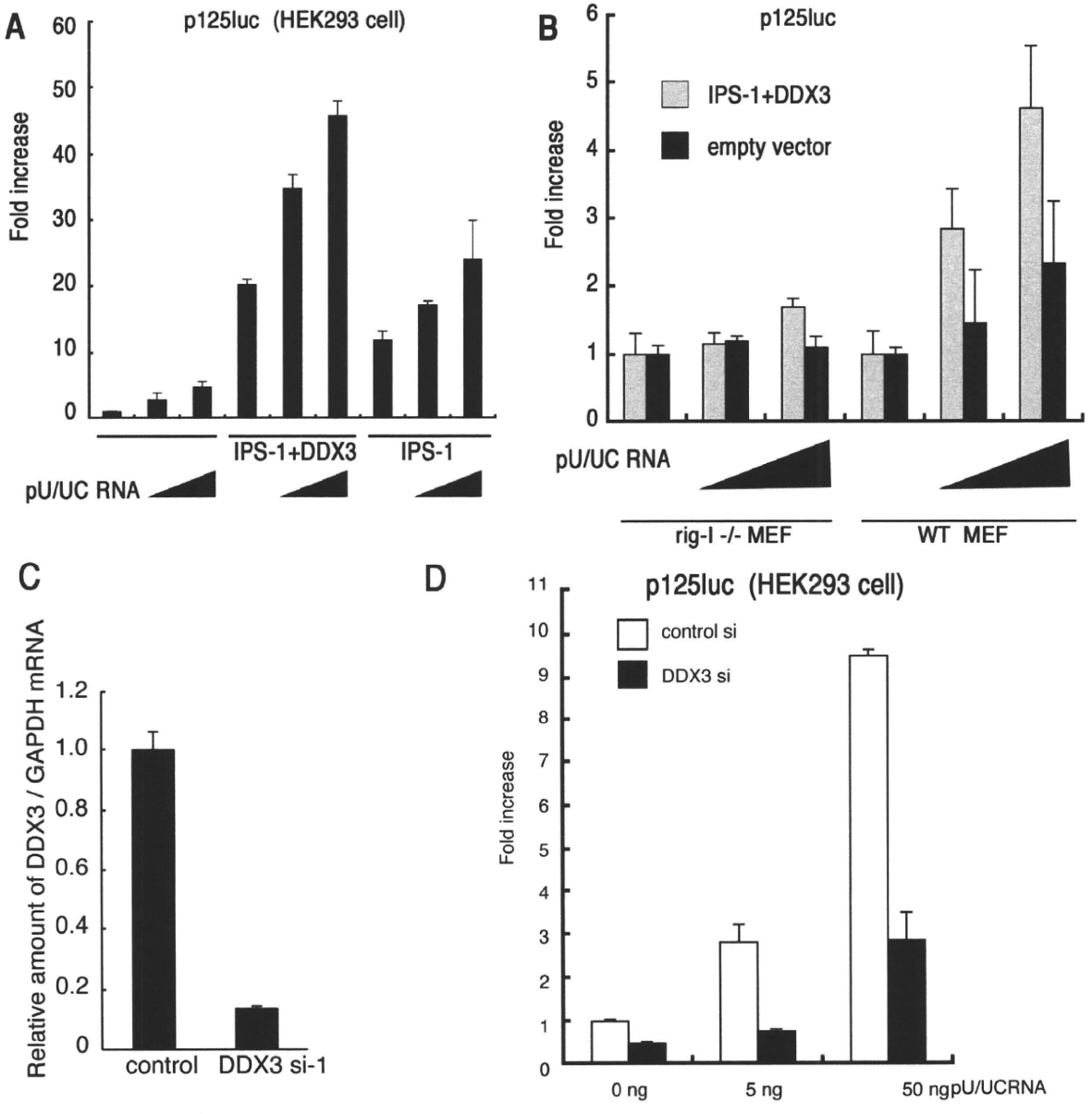


**Figure 2. DDX3 is a positive regulator of IPS-1-mediated IFN promoter activation.** (A) IFN-β induction by polyU/UC is augmented by DDX3. IPS-1 (100 ng), DDX3 (100 ng) and p125luc reporter (100 ng) plasmids were transfected into HEK293 cells in 24-well plates with or without the HCV 3′ UTR poly U/UC region (PU/UC) RNA (0, 25 or 50 ng/well), synthesized *in vitro* by T7 RNA polymerase. HCV RNA-enhancing activation of IFN-beta promoter was assessed by reporter assay in the presence or absence of the DDX3-IPS-1 complex. (B) RIG-I is essential for the DDX3/IPS-1-mediated IFN-promoter activation. MEF from wild-type and RIG-I −/− mice were transfected with plasmids of IPS-1, DDX3 and p125luc as in panel A, and stimulated with polyU/UC (0, 25 or 50 ng/well). Reporter activity was determined as in panel A. (C) Knockdown of DDX3. Negative control or DDX3 targeting siRNA (20 pmol), DDX3 si-1, was transfected into HEK293 cells, and after 48 hrs, expression of endogenous DDX3 mRNA was examined by real-time RT-PCR. DDX3 si-1-mediated down-regulation of the DDX3 protein was also confirmed by Western blotting (data not shown). (D) DDX3 enhances RIG-I-mediated IFN-beta promoter activation induced by polyU/UC. DDX3 si-1 or control siRNA was transfected into HEK293 cells with reporter plasmids (100 ng). After 48 hrs, cells were stimulated with polyU/UC (5~50 ng/ml) with lipofectamin 2000 reagent for 6 hrs, and activation of the reporter p125luc was measured. The results are representative of at least two independent experiments, each performed in triplicate.
doi:10.1371/journal.pone.0014258.g002